CHEMICAL DEGRADATION AND CHARACTERIZATION OF BACTERIAL CELLULOSE UNDER DIFFERENT CONDITIONS

by
Fulya Şahin

Submitted to Graduate School of Natural and Applied Sciences
in Partial Fulfillment of the Requirements
for the Degree of Master of Science in
Biotechnology

Yeditepe University
2022

CHEMICAL DEGRADATION AND CHARACTERIZATION OF BACTERIAL CELLULOSE UNDER DIFFERENT CONDITIONS

APPROVED BY:

Assoc. Prof. Dr. Ali Özhan Aytekin ……
(Thesis Supervisor)
(Yeditepe University)

Assist. Prof. Dr. Mehmet Hikmet Üçışık ……
(Yeditepe University)

Assist. Prof. Dr. Işık Çoban ……
(Medeniyet University)

DATE OF APPROVAL: ..../..../2022

I hereby declare that this thesis is my own work and that all information in this thesis has been obtained and presented in accordance with academic rules and ethical conduct. I have fully cited and referenced all material and results as required by these rules and conduct, and this thesis study does not contain any plagiarism. If any material used in the thesis requires copyright, the necessary permissions have been obtained. No material from this thesis has been used for the award of another degree.

I accept all kinds of legal liability that may arise in case contrary to these situations.

Name, Last name Fulya Şahin

Signature ……

ACKNOWLEDGEMENTS

Firstly, I would like to express my sincere gratitude to my thesis advisor Assoc. Prof. Dr. Ali Özhan Aytekin for his support and guidance through my thesis studies. I appreciate all the help, and opportunities he has provided to me.

I would like to express my gratitude to Assist. Prof. Dr. Mehmet Hikmet Üçışık and Prof. Dr. Fikrettin Şahin for their support through TEM and AFM analysis. Also, I would like to thank all lab members in the Process Lab in Ferhatpaşa for their support and help during my study, especially Neslihan Kayra, Burcu Şirin, and Sevda Arısoy. Additionally, I am thankful to Dr. Pınar Akkuş for her contribution and support in AFM, SEM, and TEM analysis.

Moreover, I would like to thank my friends Ali Körükmez, Gürkan Yaman, Recep Balıkçı and Derya Garip for their support, patience and time. In addition, I would like to thank my family, Olcay Şahin, Ayşe Şahin, and İbrahim Şahin for their endless belief.

The last but not least, I would like to thank to my Biomerieux TR Supply Chain family; Müge Önder Karagöz, Yalçın Kara, Yunus Emre Bulut, Derya Özcan and for their support.

ABSTRACT

CHEMICAL DEGRADATION AND CHARACTERIZATION OF BACTERIAL CELLULOSE UNDER DIFERENT CONDITIONS

Cellulose which is composed of ringed D-glucose monomers with β-1,4 glycosidic bond is the structural component of green plants, algae, and oomycetes. Bacterial cellulose is a secondary metabolite secreted by a variety of bacteria strains such as *Acetobacter* genera, *Rhizobium*, *Sarcina*, and *Agrobacterium*. *Gluconacetobacter xylinum* which is formerly as known *Acetobacter xylinum* is the most studied organism in cellulose production. *Acetobacter* genera produce cellulose pellicles and ribbons that are formed by microfibrils. Bacterial cellulose has an ultrafine network structure besides having ribbon-like microfibrils. The reticulated three-dimensional network structure of BC endows it with significant wet tensile strength, the great capability of holding water, and remarkable stability of suspension alongside being permeable, flexible, elastic, and durable. Therefore, it is widely used in the food industry, textile industry, electronic devices, drug delivery, tissue engineering, and surgical materials. The degradation of bacterial cellulose can be chemically, mechanically, and/or enzymatically. As a result of the degradation, bacterial cellulose is reduced in size up to the nanoscale. Bacterial cellulose, cellulose nanofibers (CNFs), and cellulose nanocrystals (CNCs) are the main nanocellulose types. In this study, the purpose is the chemical degradation of bacterial cellulose, which is produced by *Gluconacetobacter xylinus* FC01 strain, under different conditions including solvent pretreatment, liquid nitrogen degradation, autoclave pretreatment, and sulphuric acid degradation. The degraded samples are characterized by SEM, TEM, AFM, FT-IR, and DSC. The nanofibril structures were observed by SEM. According to TEM results, spherical nanocrystals and nanofibrils can be observed. The average length and width of samples ranged between 312.12-700 nm, and 9.09-27.27 nm. AFM images indicated 90% autoclave pretreated sample degraded into nanocrystals, 65% and 40% acid treated samples degraded into nanofibrils, and solvent pretreated with 40% acid with autoclave treated sample degraded into spherical nanocrystals. FT-IR demonstrated that OH stretching, C=C vibration, C-OH bending of samples changed due to the structural deformations. The crystallization and melting point showed distinct alterations due to the structural changes in the samples.

ÖZET

BAKTERİYEL SELÜLOZUN FARKLI KOŞULLAR ALTINDAKİ DEGREDASYONU VE KARAKTERİZASYONU

Selüloz, β-1,4 glikozidik bağ ile halkalı D-glukoz monomerlerinden oluşan, yeşil bitkiler, algler ve oomisetlerin yapısal bileşenidir. *Acetobacter* genera, *Rhizobium*, *Sarcina* ve *Agrobacterium* gibi çeşitli bakteri suşları tarafından salgılanan sekonder bir metabolittir. Eskiden Acetobacter xylinum olarak bilinen *Gluconacetobacter xylinum*, selüloz üretiminde en çok çalışılan organizmadır. *Acetobacter* cinsi, mikrofibrillerden oluşan selüloz pelikülü ve şeritler üretir. Bakteriyel selüloz, şerit benzeri mikrofibrillere sahip olmasının yanı sıra ultra ince ağ yapısına sahiptir. Bakteriyel selülozun ağsı üç boyutlu ağ yapısı, ona önemli bir ıslak çekme mukavemeti ve su tutma kabiliyeti verir. Bakteriyel selüloz geçirgen, esnek, elastik ve dayanıklı olmasının yanı sıra olağanüstü süspansiyon stabilitesine de sahiptir. Bu nedenle gıda endüstrisinde, tekstil endüstrisinde, elektronik cihazlarda, ilaç taşıyıcı sistemlerinde, doku mühendisliğinde ve cerrahi malzemelerde yaygın olarak kullanılmaktadır. Bakteriyel selülozun bozunması kimyasal, mekanik ve/veya enzimatik olabilir. Selüloz nanolifleri (CNF) ve selüloz nanokristalleri (CNC) başlıca nanoselüloz türleridir. Bu çalışmada amaç, *Gluconacetobacter xylinus* FC01 suşu tarafından üretilen bakteriyel selülozun solvent ön işlemi, sıvı nitrojen bozunması, otoklav ön işlemi ve sülfürik asit bozunması gibi farklı koşullar altında kimyasal olarak parçalanmasıdır. Bozulmuş numuneler, FT-IR ve DSC sonuçlarıyla desteklenen SEM, TEM ve AFM ile karakterize edilir. SEM ile nanofibril yapıları gözlendi. TEM sonuçlarına göre de küresel nanokristaller ve nanofibriller gözlemlenebilir. Ayrıca, numunelerin ortalama uzunluk ve genişlikleri 312.12-700 nm, 9.09-27.27 nm arasında değişmektedir. AFM görüntüleri, %90 otoklavda ön işleme tabi tutulmuş numunenin nanokristallere ayrıştığını, %65 ve %40 asitle işlem görmüş numunelerin nanofibrillere ayrıldığını ve %40 asitle solvent ön işleme tabi tutulmuş ve otoklavla işlenmiş numunenin küresel nanokristallere indirgendiğini göstermiştir. FT-IR, yapısal deformasyonlar nedeniyle numunelerin OH gerilmesi, C=C titreşimi, C-OH bükülmesinin değiştiğini göstermiştir. Son olarak da kristalleşme ve erime noktaları, numunelerdeki yapısal değişikliklere bağlı olarak belirgin değişiklikler göstermiştir.

TABLE OF CONTENTS

LIST OF FIGURES

LIST OF TABLES

LIST OF SYMBOLS/ABBREVIATIONS

α	Greek letter ‘alpha’
β	Greek letter ‘beta’
μ	Greek letter ‘mu’
μL	Microliter
AFM	Atomic force microscopy
BC	Bacterial cellulose
BCNC	Bacterial cellulose nanocrystal
CNC	Cellulose nanocrystal
CNW	Cellulose nanowhisker
dH_2O	Distilled water
DMA	Dimethylacetamide
HCl	Hydrochloric acid
H_2SO_4	Sulphuric acid
LiCl	Lithium chloride
M	Molarity
mL	Milliliter
NaOH	Sodium hyroxide
nm	Nanometer
PC	Plant cellulose
SCNC	Spherical cellulose nanocrystal
SEM	Scanning electron microscopy
TEM	Transmission electron microscopy
v/v	Volume per volume
w/v	Weight per volume
XRD	X-ray Diffraction

1. INTRODUCTION

1.1. CELLULOSE

In 1838, Anselme Paven discovered cellulose, and the celluloid product patented by Hyatt Brothers in 1870 [1]. Approximately, $1.5x10^{12}$ tons of annual biomass is represented by cellulose. Therefore, on the earth, cellulose is stated as the most abundant material and organic polymer. In the last decade, cellulose attracts scientific attention due to its specific structure. Cellulose which is composed of ringed D-glucose monomers with the β-1,4 glycosidic bond is a structural component of green plants, algae, and oomycetes [2,3]. It constitutes the plant cell wall and plays an integrative role in the stiffness, uprightness, and stability of plants [4]. In the formation of a glycosidic bond, carbon 1 of the glucose ring is linked with adjoining ring carbon 4, in this way β-1,4 glycosidic bond is established. Furthermore, the polymerization degree 'n', which ranges from 10000 to 15000 monomers, depends on the source of cellulose. The polymerization degree is also related to molecular weight such as the higher n presents the greater molecular weight. In addition, cellulose involves the methanol ($-CH_2OH$) group at the sixth carbon and hydroxyl (-OH) groups at the second and third carbon. The physical property of cellulose is governed by hydroxyl groups and their capability of making hydrogen bonds between the chains. Also, the linear configuration of the cellulose results from the stabilization of the linkage formed by hydrogen bonding between the hydroxyl group and the oxygen molecules of the adjacent ring. Besides, intermolecular forces such as van der Waals and hydrogen bonding boost the aggregation of diverse cellulose chains and induction of fibril formation [5,6]. The axial stiffness of cellulose fibrils obtained by the network of intra- and intermolecular forces, and their high cohesive energy make cellulose an insoluble polymer, even though hydroxyl and methanol groups are hydrophilic [7]. The cellulose fibrils have regions following an arrangement of the order. For instance, crystalline regions are highly ordered due to the glucose units' interactions, whereas amorphous regions are low ordered [8].

In addition, different crystal forms are existed such as cellulose I, cellulose II, cellulose III, and cellulose IV. To begin with, cellulose I is called native cellulose found in the plant cell walls. It is also convertible into cellulose II and cellulose III besides being metastable. Cellulose II which is the most stable can be acquired by sodium hydroxide treatment of

cellulose I, the process called mercerization. Additionally, while cellulose I is treated with liquid ammonia or anhydrous ethylamine cellulose III is prepared. There are two polymorphs in cellulose I as known monoclinic (Iβ) and triclinic (Iα) unit cells. The triclinic structure Iα is enriched in cellulose formed by algae and bacteria in the meantime, it can be converted to monoclinic structure (Iβ) via hydrothermal alkaline treatment. On the other side, monoclinic units (Iβ) are predominantly found in cellulose produced by higher plants and the ratio of Iα/ Iβ is dependent on cellulose origin [9–12]. The crystal structure of cellulose has been examined by several methods, for instance; 13C solid-state nuclear magnetic resonance spectroscopy, X-ray diffraction (XRD), Fourier transform infrared spectroscopy, and neutron diffraction analysis [11].

From the morphological point of view, cellulose has a prominent hierarchy of morphology such as elementary fibrils, microfibrils, and microfibrillar bands. The lateral dimensions ranging from 1.5 nm to 3.5 nm belong to elementary fibrils, from 10 nm to 30 nm are connected to microfibrils and thereabouts 100 nm is associated with microfibrillar bands [13].

The various parameters make cellulose a significant molecule. For instance, the number of hydrogen bonds, the lengths of chain, functional group, and chain length distribution, and the crystallinity. Also, the property of cellulose is associated with the isolation process because of alteration in the physico-mechanical characteristics of cellulose [14]. To exemplify, cellulose obtained from plants comprises impurities such as lignin and hemicellulose in different percentages regarding the source and thus, it is crucial to remove these structures by chemical treatments. The sulfite, organosolv, and Kraft processes are known important pulping or processing technologies in order to separate cellulose from biomass [15]. Among the pulping technologies, Kraft has mostly utilized the method whereas it has drawbacks such as decomposition of lignin and hemicellulose, usage of high pH and temperature, and releasable organic compounds that cause water contamination. Recently, in order to overcome these drawbacks, ionic liquids and green solvents are utilized to dissolve and process cellulose [16].

On the other side, the cellulose derivatives can be obtained from modifications in the highly reactive hydroxyl group (-OH), desired characteristics, or intensification some of its traits are rendered through controlled reactions [17]. There are different types of cellulose

derivatives whose properties are associated with the substituent groups; hydroxypropyl methylcellulose (HPMC), carboxymethyl cellulose (CMC), cellulose xanthate (CX), and cellulose nitrate (CN) are the examples of cellulose derivatives. Initially, hydroxypropyl methylcellulose (HPMC) is produced by the reaction of methyl chloride, sodium chloroacetate, and cellulose in the alkaline medium. It is also known as a hydrophilic polymer having biodegradable properties. In addition, it is used as a gelling agent and its dişation and thickening traits enable its usage in controlled drug release [18]. The carboxymethyl cellulose (CMC) is the result of the reaction between cellulose and sodium monochloroacetate (ClCH2-COONa) in the sodium hydroxide (NaOH) containing medium. It is used for medical applications, dyes, food, and anti-foaming surfactant agent [19]. As a result of the cellulose and carbon disulfide in the caustic medium, cellulose xanthate (CX) is able to be produced. It is used as heavy metal adsorbent due to its high capasity for ion exchange. It is also a hydrophobic molecule and insoluble in water. Additionally, in the molecule sulfur content is high, therefore sulfide interactions can occur [20]. The last but not least, cellulose nitrate (CN), which is one of the cellulose derivatives, is called nitrocellulose. It is formed by nitrating cellulose with the help of sulfuric acid and nitric acid mixture. As a consequence of fewer hydroxyl groups, cellulose nitrate does not aggregate due to hydrogen bonding. The nitrocelluloses are mainly used for explosive production [21]. The cellulose-based composites and cellulose derivatives are widely utilized in several areas especially the paper industry, purification of water, medical engineering, agriculture, cosmetics, foodstuff, and pharmaceutical area [22].

Apart from all about cellulose, bacterial cellulose (BC) which is produced by various bacterial strains has higher purity (without lignin, hemicellulose, and other biomass compounds) and greater crystallinity than plant cellulose [23–25]. Additionally, it is stated that although bacterial and plant cellulose has the same β-1,4-glucans, bacterial cellulose has 2000-6000 degree of polymerization while plant cellulose has 13000-14000 polymeric units [26]. BC has also a more homogeneous structure than plant origin. Moreover, it is indicated that bacterial cellulose has a higher surface area and porosity owing to the interconnection of the nanofibril network, that's why bacterial cellulose possesses an improved adsorption capacity of liquid. Therefore, BC gains more attention in the medical area such as skin regeneration, the implant of tissue, and medical device development since it is biocompatible, transparent, biodegradable, and non-toxic material [27,28].

1.2. BACTERIAL CELLULOSE

Bacterial cellulose, which is known as cellobiose, is a secondary metabolite perspired by a variety of bacteria strains such as *Acetobacter* genera, *Rhizobium*, *Sarcina*, and *Agrobacterium* [29]. It is considered an extracellular glucose polymer. It has an ultrafine network structure besides having ribbon-like microfibrils. The reticulated three-dimensional network structure of BC endows it with significant wet tensile strength, the great capability of holding water, and remarkable stability of suspension alongside being permeable, flexible, elastic, and durable. Also, it is reported that *Gluconacetobacter*, *Achromobacter*, *Alcaligenes*, *Azotobacter*, *Salmonella*, and *Aerobacter* are able to synthesize exopolysaccharides as microbial cellulose. While *Agrobacterium* and *Rhizobium* generate short fibrils, *Acetobacter* genera produce cellulose pellicle and ribbons formed by microfibrils [30]. Furthermore, although there have been sequenced *Gluconacetobacter* (Komatagaeibacter) species that are called BC producers, there were completely sequenced species such as *K. Xylinus* E259, *K. medellinensis* NBRC 3288, *K. nataicola* RZS0111, and *Gluconobacter oxydans* DSM 3504. In addition, *Gluconacetobacter xylinum* which is formerly known *Acetobacter xylinum* is the most studied organism in cellulose production [31,32].

1.3. ACETOBACTER XYLINUM AND BACTERIAL CELLULOSE PRODUCTION

Acetobacter xylinum is a non-pathogenic, Gram-negative soil bacterium that is identified in 1886 by Brown [33]. It is an ideal cellulose producer bacteria. This organism is also found in rotten vegetables and fruits whereas it is acquired from pellicle that is on the surface of beer [34]. There are various considerations why microorganisms produce cellulose. The first one is protecting themselves from ultraviolet and the second one is that synthesized pellicle keeps them close to the culture surface. Additionally, it is assumed that they generate a cage that enables nutrient intake easily while they are protected from heavy metal ions or enemies [35]. Also, *Acetobacter xylinum* metabolizes glucose and other sugars such as fructose or sucrose in the process of cellulose production. The biochemical pathway of cellulose synthesis consists of several steps including cellulose production and

extracellular fibril crystallization. Firstly, glucokinase converts glucose into glucose-6-phosphate then, phosphoglucomutase turns glucose-6-phosphate into glucose-1-phosphate. Afterward, UDP-glucose pyrophosphorylase takes part in the reaction and UDP-glucose is obtained from glucose-1-phosphate. Lastly, cellulose synthase which is found in the cytoplasmic membrane and converts UDP-glucose into a secondary metabolite called cellulose with the help of polymerization into a long unbranched β-1,4 glucan chain with $(C_6H_{10}O_5)n$ formula. At the end of the process, Cellulose I and Cellulose II are generated by *A. xylinum*. While cellulose I presents the ribbon-like structure of cellulose, Cellulose II infers the thermodynamically stable polymer as can be seen in Figure 1.1. [36]. Then, protofibrils pass through the bacterial cell wall. Hence, generated microfibrils that are held by inter- and intra-chain hydrogen bonding, which can be described in Figure 1.2., generate the web-shaped fibrous network and this network includes well-arranged three-dimensional nanofibers which form the hydrogel film having porous and large surface features [37,38].

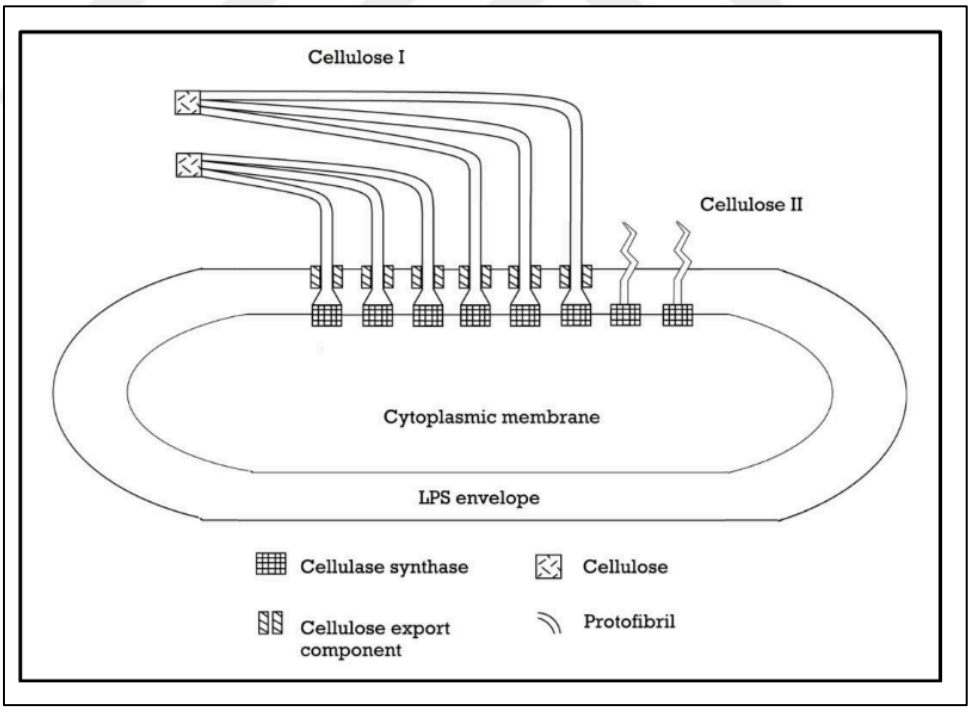

Figure 1.1. Cellulose microfibrils synthesized by *A. xylinum* [16]

In the condition of using sucrose and maltose as a carbon source instead of glucose to produce cellulose, hydrolysis of disaccharides become the first step of the process to gather

fructose and glucose [39]. Besides, this process is controlled by operon (bacterial cellulose synthase operon, bcs) and cyclic diguanylic acid (c-di-GMP) of cellulose synthase regulates the cellulose formation [40]. In the presence of c-di-GMP, which is a signaling molecule, cellulose synthase becomes activated and indicates enzyme activity since c-di-GMP is recognized by effector proteins such as transcription factors, and exopolysaccharides synthases [41]. In addition to that, cellulose synthase is linked with membrane protein called c-di-GMP binding protein which binds cellular cyclic diguanylic acid and potassium concentration modulates the equilibrium among free and bounded c-di-GMP [42]. Also, *A. xylinum* is able to conduct oxidation of carbohydrates by using the pentose-phosphate cycle as well as it performs the Krebs cycle for the oxidation of acetate-derived carbohydrates, proteins, and fat while it lacks phosphofructose activity that is crucial for glycolysis [43].

In the cellulose biosynthesis, bcsABCD operon which is identified in *Acetobacter xylinus* is implicated. In vivo, bcsA, bcsB, bcsC, and bcsD are required for utmost cellulose production while BcsA and BcsB genes are significant for BCS activities in vitro. BcsD and BcsC genes are responsible for the exportation and packaging of glucan molecules at the cell surface. The fibril production is interrupted, if BscC is mutant. Also, the production of cellulose decreases approximately forty percent if BcsD is mutant. Addition to that, there is eng (renamed as bcsZ), ccpA and bglX genes in the bcs locus of *K. xylinus*. While bcsZ and ccpA are upstream of the bcsABCD, the downstream is represented bglX. The ccpA gene is charged with cellulose production and its name is arisen from cellulose complementing protein A. The expression of BcsB and BcsC are affected by ccpA gene which is able to interact with BcsD. Therefore, it assists the formation of crystalline ribbons from the arrangement of glucan chains. The endonuclease and β–glucosidase which attends the hydrolysis of β-D-glucans are the products of bcsZ and bglX separately [44–50].

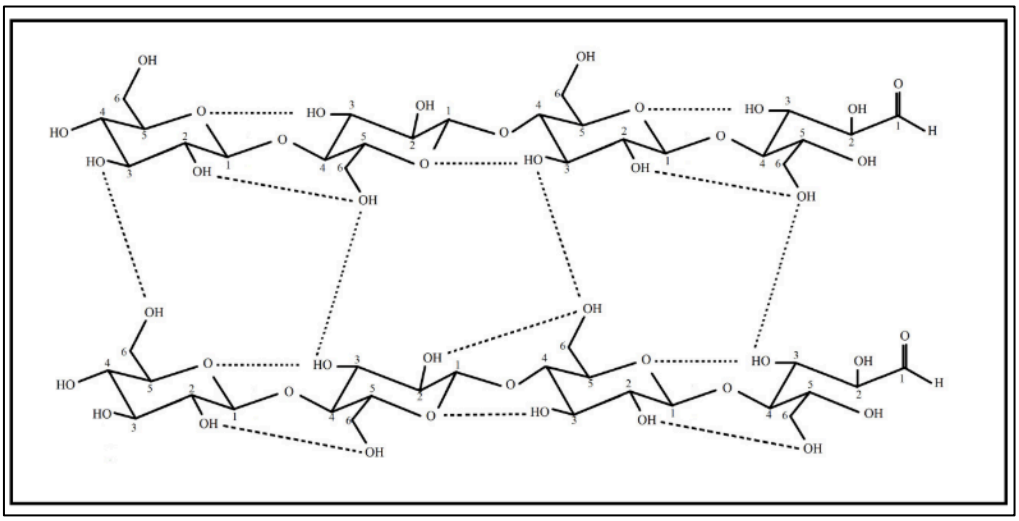

Figure 1.2. Inter- and intra-chain hydrogen bonding of BC [17]

The bacterial cellulose synthesis is able to be affected by several parameters, for instance; carbon and nitrogen source, pH and temperature influence the process. The effect of carbon sources is stated that the yield of produced cellulose is 92 percent, 15 percent, 3 percent, 11 percent, 14 percent, and11 percent when D-fructose, D-galactose, D-mannose, D-xylose, L-arabinose, and L-sorbose are used as monosaccharides. Also, sucrose has a yield of 33 percent while lactose and maltose are reported at 16 percent and 7 percent. The yield is 100 percent in the case of glucose consumption while D-arabitol and D-mannitol are indicated as 620 and 380. All in all, except for these two carbon sources, glucose has the max yield of production. By the way, when they used glucose in a low concentration such as less than 15g/l, it results in better productivity. Also, citrate is used as a carbon source, and the yield is reported as twenty percent and it is metabolized by *A. xylinum* after the glucose as glucose and citrate are found together [51]. The optimal pH of the process is generally accepted at pH 4-7 for *A. xylinum*, it is also considered that a pH lower than 7 is significant for the production [52]. 25-30℃ or 28-30℃ is the optimal growth temperature for a better cellulose yield. Moreover, corn steep liquor that includes lactate is more effective in cellulose production than peptone, yeast extract, and tryptone due to the fact that containing lactate. In addition, it is demonstrated that there are two amino acids such as methionine and glutamate are essential for the growth of cells and the generation of cellulose. Last but not least about cellulose production is the vitamins such as riboflavin, pyridoxine, nicotinic acid, pantothenate, and biotin. Even though pyridoxine, nicotinic

acid, and biotin have a positive effect on the production of cell growth, pantothenate and riboflavin have contradictory reports about their effects [30,53].

Furthermore, there are commercial media for the production of BC. The identification of suitable media is crucial to procuring high products of fermentation. The chemically defined (synthetic) media is composed of known concentrations of chemicals, but then complex media has formed a component of natural sources in undefined concentrations. There are varied media nominated for BC production. For instance; H-S ascorbic acid medium (HSA), modified HS media, altered HS media, Hassid Barker medium (HB), acetate buffered medium, Yamanaka's medium, Zhou's medium, Son medium, Park medium, M1A05P5 medium, super optimal broth with catabolite repression (SOC) medium, CSL-fructose medium, fermentation medium, Joseph medium and fructose corn step solid media [54]. However, the mentioned media above are expensive for the industrial level of production. Therefore, in recent years, industrial wastes are included in the scope of BC production to overcome the high cost of nutrients [55,56]. There are several types of industrial wastes such as agroindustrial, brewery, sugar, and textile industries. The sugar cane juice, peels of orange, lemon, mandarin, and grapefruit and pineapple residues are utilized as complex mediums. The molasses of black strap and brewery, corn steep liquor, and pomace of apple with sugar cane are example of brewery industrial wastes used as the complex media. In the sugar industries, sweet lime pulp waste, hot water extract, and sugarcane jaggery scum are exploited as synthetic media. As a result of textile mills, carob, and haricot bean medium, the biomass of waste yeast, wastewater of lipid fermentation and waste glycerol are in use for BC production [54].

The different cultivation methods play an important role in BC characteristics and application. According to current studies, BC is able to be obtained by several culture conditions including static, agitated, and bioreactor cultures. The traditional method in BC production is known as static culture. The static culture is widely used in lab-scale BC production due to its low shear force and its simplicity. The nutrients are placed into the container and it is incubated for 1-14 days at appropriate pH (4-7) and temperature (28°C-30°C). In this culture, BC is placed on the gas-liquid phase in the form of a hydrogel sheet. Addition to that, the thickness of the BC pellicle is associated with culture time. Besides, the air-liquid surface area is related to BC production since BC is generated on the surface of media [57]. Moreover, BC produced from this technique has

biocompatibility and biodegradability features that enable its medical applications. There are numerous advantages of static culture in terms of tensile strength, resistance to tearing, elastic modulus, the permeability of water, the capacity of binding, and compact texture [58]. However, the productivity is low due to the surface area of the container. Likewise, it is stated that when pellicle thickness attains a certain level, the rate of production decreases owing to inadequate nutrients and oxygen [59]. In order to overcome the high cost and low production rate of static culture, the agitation culture method is proposed. In this method, the supply of oxygen is aimed to optimize since excessive oxygen and insufficient oxygen lead to less BC generation. The BC is produced in different structures such as spheres, pellets, ellipsoidal, irregular masses, and suspension of fibrous [60]. The duration of culture time, speed of rotating, type of agitator, and additives are the factors determining the quantity, size, and shape of BC [57]. For instance, a sphere like BC is formed in the agitated culture in the lack of additives. Also, inoculation volume and culture time have an impact on sphere-like BC size and quantity. For example, the larger inoculum leads to the more spherical BC. Likewise, as the duration of culture time increases, the greater BC spheres can form [57,61]. The drawback of this method is the generation of non-cellulose mutants, thereby, the productivity decreases gradually with the genetic instability [59,62]. When static and agitated cultures are compared, BC in agitated culture has lower crystallinity and polymerization degree. Also, it is considered that the capacity of water holding and viscosity of the suspension is higher than static culture due to the fact that it has lower Young's modulus and cellulose Iα content [63]. With need for low production cost, high productivity, short duration time of cultivation, and wide application and also the achievement of production on an industrial scale, several bioreactor cultures are introduced. These bioreactors are classified in the manner of their function such as BC produced under oxygen-rich air, with the help of a rotating disc and through the support of biofilm [64]. In this cultivation method, different forms of BC can be produced depending on the bioreactor type. For instance, the elliptical pellet is acquired as a result of an airlift bioreactor whereas the rotating disc leads to a gelatinous membrane or pellet of BC. In the meantime, twisting cellulose ribbons can be procured by using a bioreactor through biofilm support [62].

1.4. APPLICATIONS OF BACTERIAL CELLULOSE

In the food industry, BC is used as a raw material for the manufacturing of nata de coco which is a popular dessert in Southeast Asia. BC was produced in static culture from coconut water serving as a carbon source. Also, it can be used as additives for foods in order to endow some properties. For instance, the stickness of pasty foods is decreased by the addition of BC in this way, their mouthfeel is improved [65]. Addition to that, it gives chewiness and juiciness to meatballs [66]. The contour of ice cream for at least 60 min is also provided by BC addition, elsewise it melts after leaving from freezer [67]. Furthermore, BC has a role in the packaging of foods. It is stated that BC including films ensures both mechanical strength and permeability of water vapor and gas [68].

In addition to that, BC is utilized in the textile industry due to the green and sustainable approaches. It is stated that BC produced from coconut water and residues of the industry is an alternative to leather in the development of fashion accessories. Also, it can be dyed and the dyeing procedure influences the flexibility and porous structure of cellulose [69]. With the development of BC-based composites, the hydrophobicity, flexibility, and mechanical properties of BC can be improved for application in the textile industry. For instance, antimicrobial features, and intense color can be incorporated into BC with biocides and acrylate epoxidized soybean oil emulsion [70].

Towards the development of flexible electronic devices, BC is also gaining attention on the basis of biodegradability, piezoelectricity, and dielectricity. For electronic applications, BC is transferred into a carbon network via the carbonization technique. In this way, it is considered as an excellent electrode material for capacitors. Furthermore, it is used in optoelectronic devices and flexible organic light emitting diodes (FOLED) [71,72]. On the other hand, it is considered that glucose fuel cells which are utilized oxygen and glucose in order to raise the current of electricity needed for medical implants are developed by BC [73].

Bacterial cellulose has core intrinsic features such as it is non-toxic, cost-efficient, mechanically stable, and biocompatible. Therefore, it is used in distinct applications, for instance, drug delivery, wound dressing, tissue engineering, and surgical materials. The anti-inflammatory, and antimicrobial drugs are loaded in BC membranes via immersion

method for maximum drug absorption For instance, gastrointestinal symptoms are caused by taking ibuprofen and diclofenac in some people, with respect to this transdermal delivery system is ensued [74]. In the release of diclofenac, bacterial cellulose is composited with Polymethanocryolyl-glycine in order to obtain a scaffold that is sensitive to pH. When pH is 2, the composite keeps the drug inside. However, it is applied to the skin which is a pH of 7.4, drug release is started within a period of 96h [75].

In oral drug delivery, famotidine and tizanidine drugs are immediately released for unmodified BC while modifications on BC alter the matrices hydrophilicity that contributes to the release of drug with the great sustaining effect drug [76]. Even, laser-sensitized magnetic nanoparticles are loaded on BC membrane to overcome limited penetration depth challenges in breast cancer treatment [77]. In addition, silver containing BC is utilized in wound dressing due to block bacterial growth. It also avoids dehydration of wound dressing, and reduces pain and discomfort by maintaining the humidity around the wound. Besides, the high water content of bacterial cellulose provides re-epithelisation at the wound site [78].

In tissue engineering, it is crucial to select the scaffolds since they adjust the growth of cells and tissues through maintaining their shape and function. The intracellular matrix of bacterial cellulose ensures being an ideal scaffold in a variety of cell types. Roman et al., indicated that porosity, the content of water, mechanical property, and bioactivity of BC influence the biomimetic features [79]. For instance, the extracellular matrix includes water between 60-80 percent depending on tissue type [80]. Therefore, the water content of BC is able to be altered by densification of BC or by adding water-soluble polymer to BC. Also, bioactivity is another important feature. Proliferation and attachment of cells are improved with distinct strategies such as the addition of silk to BC, coating with collagen or gelatin, and also adhesion peptide bioconjugations [81,82]. On the other side, porosity affects the adhesion, migration even differentiation of the cells, thus mesh density of BC fibrils plays a significant role. The migration is restricted by the high mesh density of BC, therefore porogen can be used [78,83]. Zaborowska et al. demonstrated that the addition of paraffin wax microspheres during the fermentation process results in microporous bacterial cellulose structure which is needed for osteoblast growth and mineralized tissue formation [84]. Furthermore, for cartilage or injured bone, BC scaffolds are developed with immersion in sodium hydroxide in order to promote the proliferation of cells. Similarly,

BC with hydroxyapatite induced growth and adhesion of osteoblasts on the scaffold when it is compared to the BC membrane alone [85]. Additionally, BC is a candidate material for vascular grafts. Klemm et al. showed that blood vessels smaller than 5 mm constituted similar mechanical properties and moldability to BC (BActerial SYnthesized Cellulose (BASYC)) replacing atherosclerotic coronaries [86]. Moreover, the synthetic cornea was produced from BC with polyvinyl alcohol (PVA) though BC alone was not suitable for this purpose [87]. The last but not least, when the BC membrane is oxidized and a bactericide is loaded onto it, Inoue et al. revealed that this membrane is used for dental medicine [88].

1.5. DEGRADATION OF BACTERIAL CELLULOSE

Cellulose can be reduced in size up to nanoscale with the help of various methods including chemically, mechanically, and/or enzymatically [89]. When cellulose has a nanometer range of at least one dimension, it is called nanocellulose. Bacterial cellulose, cellulose nanofibers (CNF), and cellulose nanocrystals (CNC) are the main nanocellulose types [86] as can be seen in Figure 1.3. There are several studies about the enzymatic hydrolysis of bacterial cellulose. Auta et al. conducted characterization of BC microfibrils treated cellulase from Aspergillus niger. The cellulase treatment of BC changed physical properties such as crystallinity, mechanical strength, and water holding capacity. Also, after enzyme treatment, cellulose type I in untreated BC was transformed into cellulose type II which represents amorphous regions. Microfibrils of BC were hydrolyzed into sugar monomers after enzymatic treatment [90]. Cellulase enzymes can be classified as endoglucanases (endocellulases) which are responsible for the hydrolysis of cellulose amorphous region; cellobiohydrolases (CBH) or exoglucanases which perform the cleavage of crystalline part found at the end of cellulose and cellobiose dimers (disaccharides) tetrasaccharides are generated; β-glucosidases that are for the hydrolysis of disaccharides and tetrasaccharides that are products of cellobiohydrolases [91]. Santa-Maria et al. used cellobiohydrolase (Cel7A) to degrade bacterial cellulose produced by *Gluconacetobacter xylinum* sbsp in static cultivation. As a result, microfibrils with a diameter of 3-5 nm and channels in the depth of 0.3-0.5 nm were observed at high amount of hydrolysis greater than 80 percent. Also, spherical cellulose particles were observed due to the physical aggregation of cellulose microfibrils after sonication [92]. Besides, George et al. utilized cellulase in order to produce nanocrystals of cellulose, and obtained

nanocrystals showed better mechanical and thermal features when they are compared to acid hydrolysis [93,94]. Moreover, bacterial cellulose was exposed to enzymatic hydrolysis whereas eucalyptus fibers were to acid hydrolysis according to Dominges et al. They indicated that homogenous rod-shaped nanocrystals generated from eucalyptus fibers with the help of acid hydrolysis displayed high zeta potential -(17 ± 1) mV and aspect ratio (length of 180nm and width of 5 nm) at pH equals to 6. The nanocrystals hydrolyzed enzymatically had grooves and were C-shaped with the value of zeta potential –(23 ± 2) mV [95]. Furthermore, Rovera et al. hydrolyzed bacterial cellulose using endo-1,4-β-glucanases (EGs) and cellulase to acquire bacterial cellulose nanocrystals. The cellulase enzyme treatment resulted in a higher amount of nano-scale particles around 250 nm. Also, round-shaped cellulose nanoparticles were comprised of 4-5 short whiskers (150-180 nm)[94,96].

In addition to enzymatic hydrolysis, rod-like cellulose nanocrystals can be obtained by sulphuric acid (64 percent wt) hydrolysis of native cellulose. However, Neng et al. stated that spherical cellulose nanocrystals (SCNC) can be gathered from the microcrystalline cellulose (20 μm) treated with sulphuric acid (98 percent w/w) and hydrochloric acid (37 percent w/w) mixture under ultrasonic method at 50 Hz for 10 h. They also found that ultrasonication was essential to obtain spherical nanocellulose particles, otherwise, the particles were not acquired. The hydrolysis time was another crucial parameter; if the time of hydrolysis increased, micro fragments vanished and SCNCs were regularly formed [97]. Similarly, acid hydrolysis is the most common method to reduce BC in size to nanocrystals. The hydrogen ions initially hydrolyze the amorphous or disordered region of BC by disturbing glycosidic bonds in there, and the remaining crystalline regions that are resistant to acid form crystallites [94]. To that end, sulphuric and hydrochloric acids have been widely used likewise, hydrobromic and phosphoric acids are able to be utilized. Further, CNCs produced by sulphuric or phosphoric acid are dispersible in water whereas those obtained by hydrobromic or hydrochloric acids tend to be flocculated [98]. The acid hydrolyzed cellulose is often denominated as microcrystals, microcrystallite, whiskers, microfibrils, or nanocrystals. However, cellulose nanocrystals are used for sulphuric acid treated celluloses [99]. Additonally, cotton and wood cellulose nanocrystals had 3-5 nm width and 100-350 nm length [100] while bacterial cellulose nanocrystals had ribbon-like shape with 10 nm x 50 nm dimensions depending on the condition of hydrolysis and length

can be ranged from 100 nm to various micrometers. Araki et al. stated that by using 65 percent sulphuric acid at 70 °C for 30 min, BC nanocrystals were able to be prepared [101]. Hirai et al. indicated the phase separation of BCNCs generated by 60 percent wt sulphuric acid stirred at 51 °C for 1 h. The sample then passed a mixed bed ion exchange resin column and a cellulose dialysis tube was used. As a result, isotropic and chiral nematic phases of suspensions were achieved under different NaCl conditions [99]. Vasconcelos et al. used sulphuric acid in different concentrations and different exposure times for the obtaining of BCNCs. 0.6g dried BC mixed with 60 mL acid solutions (50 percent H_2SO_4 w/w for 60 min, 50 percent H_2SO_4 w/w for 120 min, 60 percent H_2SO_4 w/w for 60 min, 65 percent H_2SO_4 w/w for 120 min, 34 percent H_2SO_4 w/w with 24 percent HCl w/w for 60 min) at 45 ◦C under the stirring condition at 500 rpm. As a result, needle-like nanostructures were obtained with a length of 622-1322 nm and a diameter of 33.7-44.3 nm [102]. On the other hand, Yan et al. prepared bacterial cellulose nanocrystals through sulphuric acid hydrolysis (80 mL of 50 wt percent) at 45 ◦C for 3 h. Then, BCNs were oxidized with 8 mL of 30 percent wt hydrogen peroxide solution. Consequently, sulphuric acid treatment ensured the removal of amorphous parts of BC and also crystalline microfibrils. Addition to that,obtained BCNs showed higher thermal stability than BC [103].

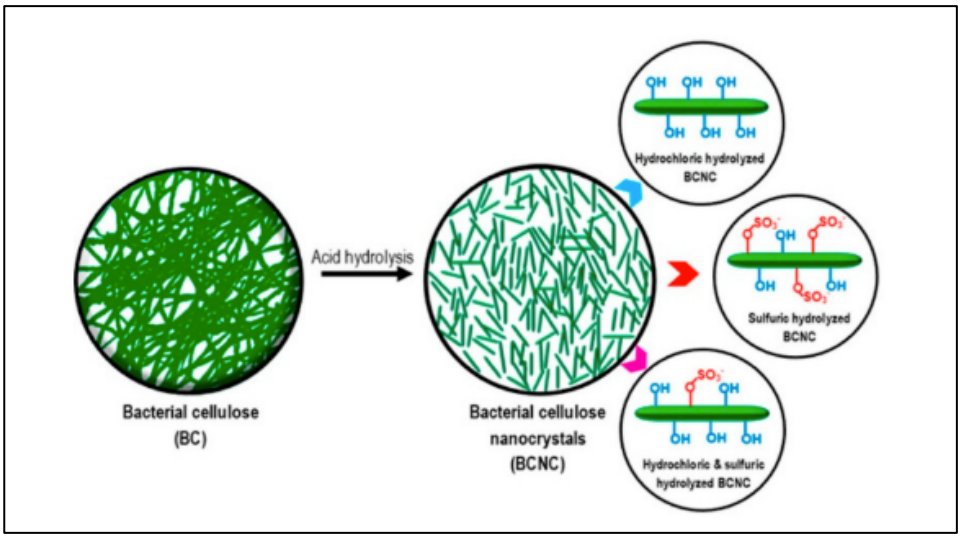

Figure 1.3. Diagram of BCNCs under different acid hydrolysis [94]

Arserim-Uçar et al. studied bacterial cellulose nanocrystals (BCNCs) from bacterial cellulose nanofibers (BCNFs). For this purpose, 40g wet BCNFs were hydrolyzed with

200 mL acid solution including sulphuric acid and hydrochloric acid. The crystallinity of BCNCs elevated when reaction temperature increased by 10°C [104]. Also, Salari et al. used both mechanical methods and acid hydrolysis in their study. Herewith, in the preparation of BCNCs, a laboratory blender was used for fragmentation of BC pellicle, then it was exposed to 50 percent w/w of 98 percent concentrated sulphuric acid at 50°C for 40 min under stirring conditions. To quench the hydrolysis, 10-fold distilled water was used. Then, ultrasonication and homogenization processes were performed. As a result, rod-like shaped nanocrystals were obtained in the size of 25±5 nm in diameter and 306±112 nm length [105].

On the other side, cellulose nanocrystals and nanofibers obtained through acid hydrolysis are referred to as cellulose nanowhiskers. The morphology of cellulose nanowhiskers (CNWs) is affected by hydrolysis time, temperature, the ratio of acid and cellulose, concentration of acid, and source of cellulose. For instance, CNWs of cotton or wood have 100-300 nm length and 5-20 nm width [106] while the length of bacterial or tunicin CNWs has assorted micrometers and 5-50 nm width [107]. Martinez-Sanz et al. performed sulphuric acid treatment (96 percent Pancreac) with a ratio of 8–10 g/L at 50 °C under different time arrivals after mechanical degradation of BC pellicles through a blender [108]. Furthermore, CNWs were used as a reinforcer of the ethylene vinyl alcohol polymer matrix in the Sanz et al. study. They prepared CNWs with the help of 50 percent (v/v) sulphuric acid at a ratio of 7g/L at 50°C for 120 h. Then, they were incorporated into EVOH matrix by electroporation in order to achieve well-dispersed BCNWs in the polymer matrix [109].

In addition, cellulose nanofibers (CNF) can be obtained from different sources by the steam explosion method. Although, cellulose fibers can be gathered by acid hydrolysis, mechanical processes such as homogenization, or the chemical and mechanical process combination. There are some advantages of the steam explosion method; during the process, fewer chemicals and less eneergy are needed. Also, it is stated that this method is called thermomechanochemical operation. Since moisture generates shear force and steam produces heat. In this way, hemicellulose in the cellulose fibers is hydrolyzed [110]. This method ensures CNFs from several materials such as pineapple leaf [111], wheat straw [112], Helicteres isora plant [113], and banana [114]. In addition to that, Saragih et al. procured cellulose nanofibers that are generated from α-cellulose of abaca fibers treated

with acid hydrolysis and alkalization with the help of autoclave at 130 °C for 15 min at the pressure of 130kPa. After the homogenization of CNFs, they were used for hydrogel development with N, N-methylene bisacrylamide (MBA) [115]. Moreover, Cherian et al. found an effective method for depolymerization and defibrillation for the extraction of nanofibrils from pineapple leaf fibers. That is the acid treatment with steam explosion [111]. However, Kaushik et al. stated that hydrochloric acid treatment and high shear homogenization after the steam explosion with alkaline media is the effective process for depolymerization and defibrillation [112]. Besides, the steam explosion can be used in pretreatment in order to decrease non-cellulosic materials such as lignin and hemicellulose. For instance, Oliveira et al. indicated that hemicellulose solubilization was achieved by steam explosion pretreatment of sugarcane straw, likewise, solubilization of lignin has resulted from alkaline treatment after pretreatment [116].

The last but not least object is the dissolution of bacterial cellulose on the dimethylacetamide/lithium chloride (DMAc/LiCl) solution. Lima et al. demonstrated that 1 percent of bacterial cellulose was dissolved in the DMAc/LiCl solvent system completely and BC pellicle became a translucent membrane. Else, bacterial cellulose lost its crystal structure and it turned into an amorphous frame [117]. In the process of dissolution, it is accepted that macrocation of $[DMAc+Li]^+$ is formed when Li^+ ions interact with oxygens in the carbonyl group of DMAc. Simultaneously, hydroxyl protons of cellulose have interacted with Cl^- ions leading to the dispersion of network chains composed of hydrogen bonds. Due to the fact that lithium and chloride ions act as ion pairs, DMAc/LiCl solvent does not exhibit chemical bond formation [118]. Additionally, Yudianti et al. stated that 8 percent (w/w) DMAc/LiCl not only enabled the BC pellicle to have excellent transparent properties but also native BC fibrillar structure vanished after exposure to this solvent system [118].

2. AIM

When distinct degradation processes are considered, in this study, we aimed that BC pellicle produced by *Gluconacetobacter xylinus* was chemically degraded under different conditions and characterized by several methods.

3. MATERIALS

3.1. CHEMICALS

Lithium Chloride (Sigma-Aldrich), Sodium Chloride (#31434, Sigma Aldrich) Dimethylacetamide (N,N Dimethylacetamide DMAc or DMA) (Sigma-Aldrich), Sulphuric Acid (H_2SO_4) (Riedel de Haen, 95-97 percent, CAS-Nr: 231-639-5).

3.2. LABORATORY DEVICES AND EQUIPMENTS

Cryo tube; mL: 2 (Isolab), Eppendorf tube; mL: 1,5, 2 (Isolab), Erlenmeyer Flask; mL: 250, 500, 1000 (Isolab), Falcon tube; mL: 15, 50 (Isolab), Graduated cylinder; mL: 10, 50, 100, 500, 1000 (Isolab), Glass bottle; mL: 50, 100, 250, 500, 1000 (Isolab), Inoculation loop (Isolab), Micropipette; µL: 1-10, 10-100, 20-200, 100-1000 (Eppendorf), Micropipette tip; µL: 10, 200, 1000 (Eppendorf, Thermo Scientific), Petri dish; 120 x 17 mm (Isolab), Serological pipette ;mL: 5, 10, 25 (SLP Life Sciences), Sonicator (Bangdelin Series 2000.2), Autoclave (Daihan Scientific), Balance Scale (Shimadzu), Centrifuge (Eppendorf 5810R, Gyrozen), Drying oven (Binder), Fume hood (Greenlife), Magnetic stirrer (Daihan Scientific), pH meter (Mettler Toledo), Water bath (Grant SUB Aqua 12 Plus, Memmert).

4. METHODS

4.1. PRODUCTION OF BACTERIAL CELLULOSE

Gluconacetobacter xylinus FC01 strain (3 percent v/v) was inoculated into defined medium M1A05P5 including glucose 10 g/L, yeast extract 10 g/L, peptone 7g/L, acetic acid 1.5 g/L and ethanol 5 g/L at pH 5.0. Microbial cultures were incubated at room temperature under static culture and produced bacterial cellulose on the surface of the erlenmeyer flask was collected. Pellicles were washed with distilled water. Then, they were treated with 2M NaOH at 80°C for 1h, with 70 percent ethanol for 24h, and with acetone for 24h respectively.

4.2. TREATMENTS OF BACTERIAL CELLULOSE PELLICLES

4.2.1. Pretreatments

4.2.1.1. *Solvent Pretreatment*

BC pellicles were pretreated with 8 percent (w/v) LiCl-Dimethylacetamide (N, N Dimethylacetamide DMAc or DMA) (Sigma-Aldrich) solution for 2 days at room temperature. After that, they were with 70 percent ethanol and washed with plenty of distilled water.

4.2.1.2. *Acid Pretreatments*

Autoclave Pretreatment with Sulphuric Acid

BC pellicle (30 percent w/v) was cut into small pieces. BC pellicle pieces (30 percent w/v) mixed with 90 percent, 65 percent, and 40 percent H_2SO_4 (Riedel de Haen, 95-97 percent, CAS-Nr: 231-639-5) solutions in bottles, were autoclaved for 15 min at 121°C and 45 min at 121°C separately. After autoclave pretreatment, distilled water was added to suspensions at a ratio of 15:1 v/v.

Room Temperature Pretreatment with Sulphuric Acid

BC pellicle (30 percent w/v) was cut into small pieces and pretreated with 90 percent, 65 percent, and 40 percent H_2SO_4 solutions at room temperature for total autoclave times such as 1h 40 min and 2h 40 min respectively. Treatment quenched with distilled water with a ratio of 15:1 v/v.

4.2.2. Degradation of Pretreated Samples

4.2.2.1. *Degradation with Sulphuric Acid*

Pretreated samples were filtrated using a 0.2 μm cellulose nitrate filter. Residues on the filter were collected with 10M NaOH solution and washed with distilled water. They were centrifuged at 8000 rpm for 20 min 3 times. They were filtrated again with the help of a 0.2 μm cellulose nitrate filter. The wet residues of 30 percent (w/v) were degraded with 65 percent H_2SO_4 solution for 2 days at room temperature. After treatment termination, samples were centrifuged at 12000 rpm for 15 min 3 times.

4.2.2.2. *Degradation with Liquid Nitrogen*

Solvent pretreated samples were ground with the help of liquid nitrogen (LN2) in mortar.

4.3. SCANNING ELECTRON MICROSCOPY

The suspensions of samples were sonicated for 30 sec (Bangdelin Series 2000.2) and mounted on a glass microscope slide. Images were executed SEM ZEISS EVO40 with an acceleration voltage of 10kV after coating samples with Au/Pd for 1 min with Leica EM ACE200 Vacuum Coater.

4.4. TRANSMISSION ELECTRON MICROSCOPY

Suspensions of samples were sonicated for 1 min and deposited on transmission electron microscope copper grid covered with carbon film (Agar Scientific, Holey Carbon Film on 200 Mesh Copper Grid) and held for 3 min. Excess liquid was carefully removed by filter

paper and samples were stained with 2 percent uranyl acetate solution (TED PELLA 19485) to enhance microscopic resolution. After drying of samples, micrographs were taken by Jeol 2100 Plus TEM with an acceleration voltage of 120 kV.

4.5. ATOMIC FORCE MICROSCOPY

Sample suspensions were sonicated for 30 sec and dropped on the glass slide surface. After drying of samples at room temperature, they were analyzed in contact mode using Si cantilever with a scanning rate of 1.0 Hz by AFM (Park Systems XE 100). XEI image processing program was used for AFM image examination.

4.6. FOURIER TRANSFORM INFRARED SPECTROSCOPY (FT-IR)

Samples were analyzed with Smart i-TR (Thermo Scientific Nicolet^{TM} iS10^{TM}). Before analyzing, samples were dried overnight. Spectra were obtained at 525 cm^{-1} and 4000 cm^{-1}.

4.7. DIFFERENTIAL SCANNING CALORIMETRY (DSC)

Samples were examined by using SETARAM Instrumentation Keep Technologies DSC 131. Samples (4-10 mg) were heated from 25 °C to 400 °C under a nitrogen atmosphere (50 mL/min). The heating rate was 10 °C /min.

5. RESULTS

The all pretreatment and treatment procedures are summarized in the Table 5.1. as can be seen below.

Table 5.1. The summary of treatment procedures

			Autoclave for 15 min			Room Temperature for 1h 40 min			Autoclave for 45 min			Room temperature for 2h 40min			
Sample	8%LiCl-DMA	Liquid Nitrogen	90% H_2SO_4	65% H_2SO_4	40% H_2SO_4	90% H_2SO_4	65% H_2SO_4	40% H_2SO_4	90% H_2SO_4	65% H_2SO_4	40% H_2SO_4	90% H_2SO_4	65% H_2SO_4	40% H_2SO_4	65%H_2SO_4 for 2 days at RT
1	+	+	-	-	-	-	-	-	-	-	-	-	-	-	-
2	+	-	-	-	+	-	-	-	-	-	-	-	-	-	-
3	-	-	-	-	-	-	-	-	+	-	-	-	-	-	+
4	-	-	-	-	-	-	-	-	-	-	-	-	-	+	+
5	-	-	-	-	-	-	-	-	-	-	-	+	-	-	+
6	-	-	-	-	+	-	-	-	-	-	-	-	-	-	-
7	-	-	-	-	-	-	-	-	-	-	-	-	+	-	+
8	-	-	-	-	-	-	-	-	-	-	-	-	-	-	+
9	-	-	-	-	-	-	-	+	-	-	-	-	-	-	+
10	-	-	+	-	-	-	-	-	-	-	-	-	-	-	+
11	-	-	-	-	-	+	-	-	-	-	-	-	-	-	+
12	-	-	-	-	-	-	-	-	-	+	-	-	-	-	+
13	-	-	-	+	-	-	-	-	-	-	-	-	-	-	+
14	-	-	-	-	-	-	+	-	-	-	-	-	-	-	+
15	-	-	-	-	-	-	-	-	-	-	+	-	-	-	+
16	-	-	-	-	+	-	-	-	-	-	-	-	-	-	+

In this study, chemically degraded bacterial cellulose samples were characterized by SEM, TEM, AFM, FT-IR, and lastly DSC as can be seen following.

5.1. SEM RESULTS

According to SEM results, there are micro fibrillar structures were observed at 1.00 K X magnification after both 45 min autoclave and 40 percent sulphuric acid pretreatment and 65 percent sulphuric acid degradation as can be seen in Figure 5.1. Scale marker represented 20μm.

It has revealed that autoclave and acid pretreatment with the acid degradation caused morphological changes in bacterial cellulose.

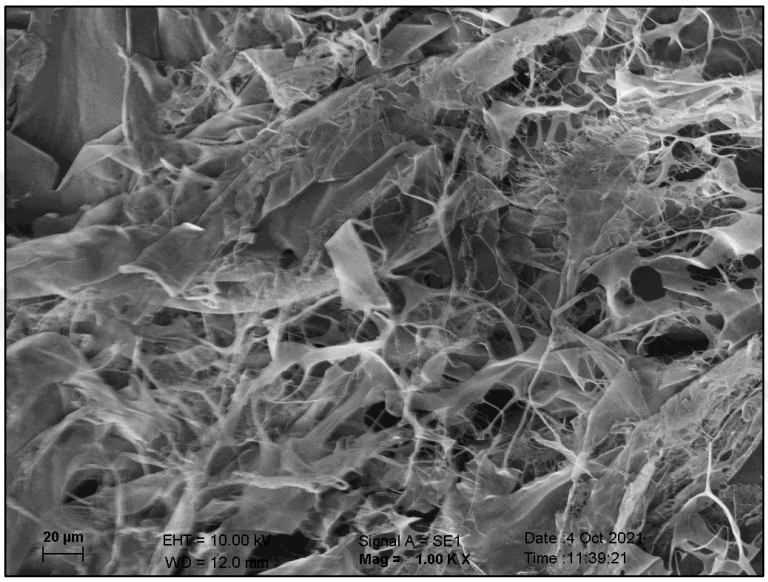

Figure 5.1. SEM Image of the sample is exposed to 40% sulphuric acid pretreatment with autoclave for 45 min at 121°C and 65% sulphuric acid degradation at room temperature for 2 days

With the increment in the sulphuric acid concentration, Figure 5.2. indicated that 65 percent sulphuric acid pretreatment with 45 min autoclave caused more degraded bacterial cellulose sample.

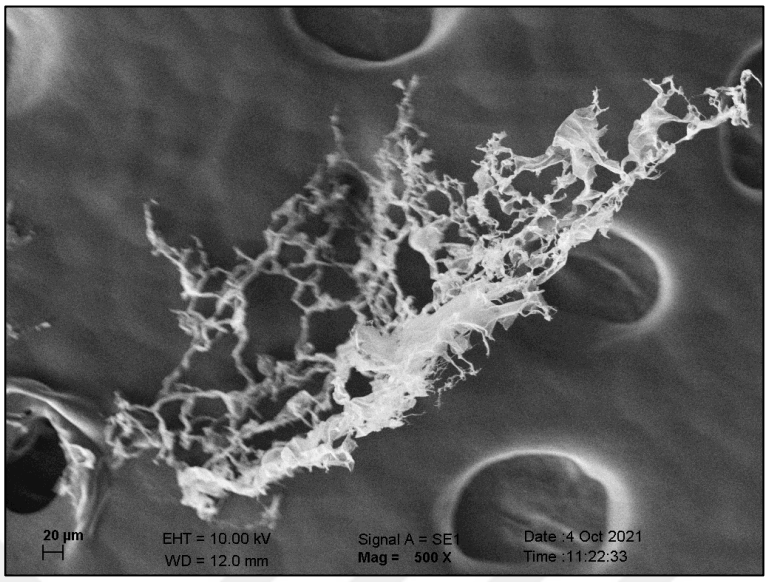

Figure 5.2. SEM Image of the sample is exposed to 65 % sulphuric acid pretreatment with autoclave for 45 min at 121°C and 65% sulphuric acid degradation at room temperature for 2 days

5.2. TEM RESULTS

Table 5.2. demonstrated a rough estimation of the bacterial nanofibrils obtained from bacterial cellulose under different conditions. According to the data on the table, pretreatments and treatments altered the width and length of nanofibrils. Although the widths of sample 8 (65 percent sulphuric acid at room temperature for 2 days), and sample 7 (65 percent sulphuric acid at room temperature for 2 h with 65 percent sulphuric acid degradation) were the same, their lengths were different for each other. In addition, sample 1 (solvent treatment with liquid nitrogen degradation) not also led to less separation between bundles of nanofibrils but also caused less degradation in terms of length. Also, autoclave prtreatment resulted in a decrease in both length and width for sample 6 and sample 4 which are exposed to 40 percent sulphuric acid. The last but not least, the length estimation of sample 6 (40 percent sulphuric acid with autoclave for 15 min at 121°C) and sample 7 (65 percent sulphuric acid at room temperature for 2 hours 40 min with the 65 percent sulphuric acid degradation for 2 days at room temperature) were close to each other. However, they were different in terms of widths.

Table 5.2. Calculated average size and length of bacterial cellulose nanofibrils.

Sample	Length (nm) (average)	Width (nm) (average)
8%LiCl-DMA + Liquid Nitrogen	700	18.18
40% H_2SO_4 @ RT 2h 40min + 65% H_2SO_4 @ RT 2days	569.69	27.27
40% H_2SO_4 with Autoclave for 15 min @ 121 °C	490.9	12.12
65% H_2SO_4 @ RT 2 days	312.12	9.09
65% H_2SO_4 @ RT 2h 40 min + 65% H_2SO_4 @ RT 2days	462.96	9.09

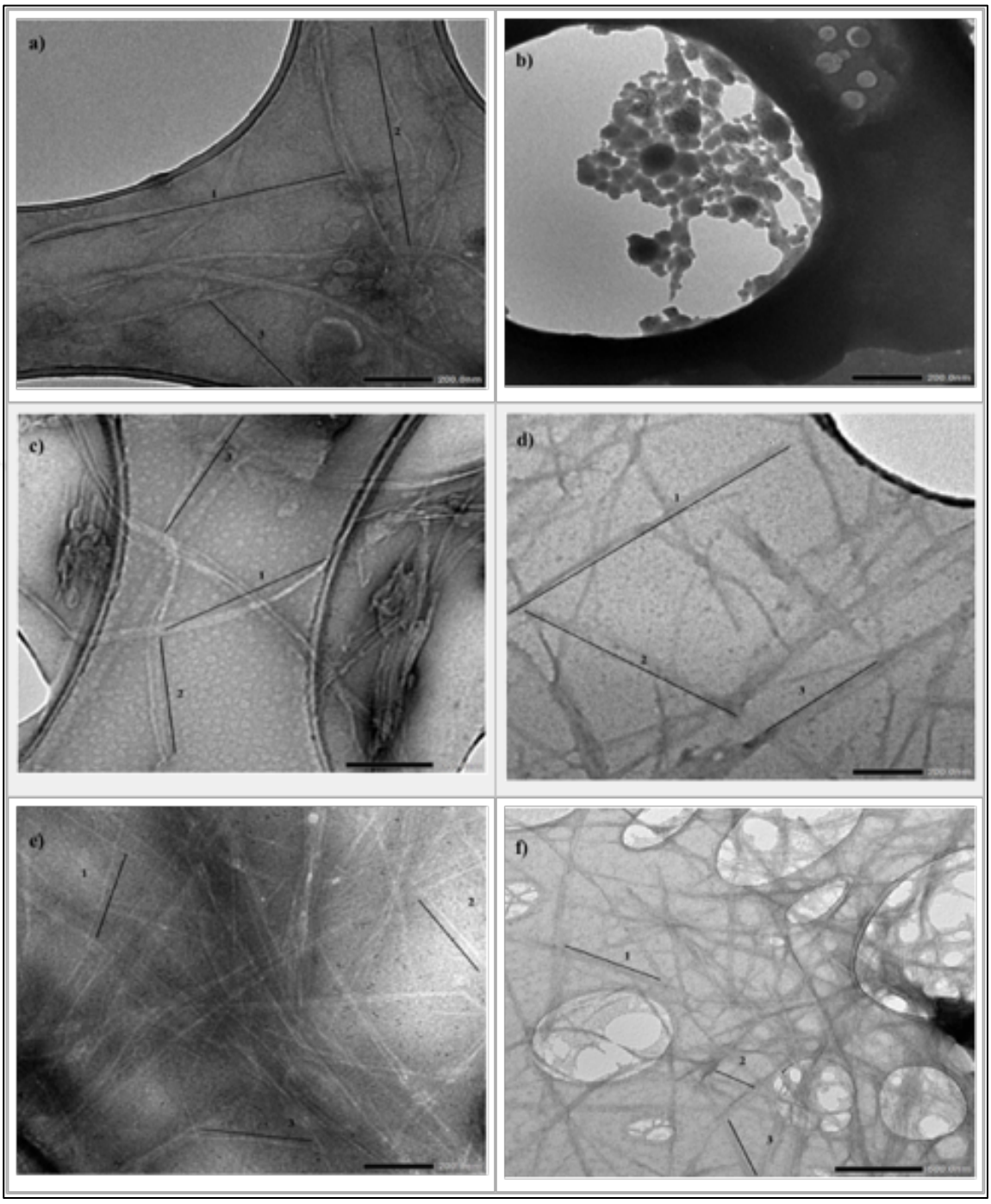

Figure 5.3. TEM Images of degraded bacterial cellulose samples under different conditions. a) sample is pretreated with solvent of 8% (w/v) LiCl-DMA for 2 days at room temperature and degraded with liquid nitrogen. b) sample is pretreated with solvent of 8% (w/v) LiCl-DMA for 2 days at room temperature and treated with 40% sulphuric acid with autoclave for 15 min at 121°C. c) sample is pretreated with 40% sulphuric acid with autoclave for 15 min at 121°C. d) sample is pretreated with 40% sulphuric acid at room temperature for 2 hours 40 min and degraded with 65% sulphuric acid at room temperature

for 2 days. e) sample is treated with 65% sulphuric acid at room temperature for 2 days. f) sample is pretreated with 65% sulphuric acid at room temperature for 2 hours 40 min and degraded with 65% sulphuric acid at room temperature for 2 days.

In Figure 5.3., sample 1 and sample 2 had distinct features in TEM images. The sphere-like bacterial cellulose nanocrystals were obtained at the end of the combination of 8 percent (w/v) LiCl-DMA solvent pretreatment and 40 percent sulphuric acid with 15 min autoclave treatment. Whereas, sample 1 showed nanofibril structures acquired from solvent treatment with liquid nitrogen degradation.

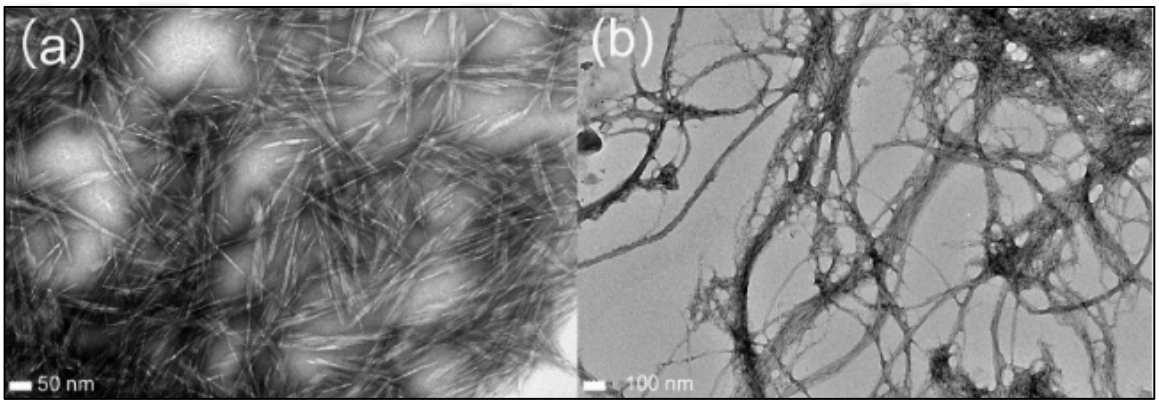

Figure 5.4. TEM Image of bacterial cellulose nanocrystals (a) and nanofibers (b) [119]

Depending upon sample 6 nanofibril structures were observed similar to sample 4, sample 8, and sample 7. The network of fibrils can be seen for sample 8 and sample 7 while rod-like and short nanofibrils were able to be seen for sample 6 and sample 4. Besides, distribution of the structures at room temperature treatments is more intensive than autoclave pretreatment. Additon to that, Figure 5.4. showed the difference between bacterial cellulose nanocrystals and nanofibers under the transmission electron microscope.

5.3. AFM RESULTS

When sample 1 and sample 2 are compared, solvent pretreatment with liquid nitrogen degradation resulted in bacterial cellulose nanofibrils, whereas solvent pretreatment with a steam explosion for 15 min via autoclave provided spherical-like nanocrystals as can be seen in Figure 5.5.

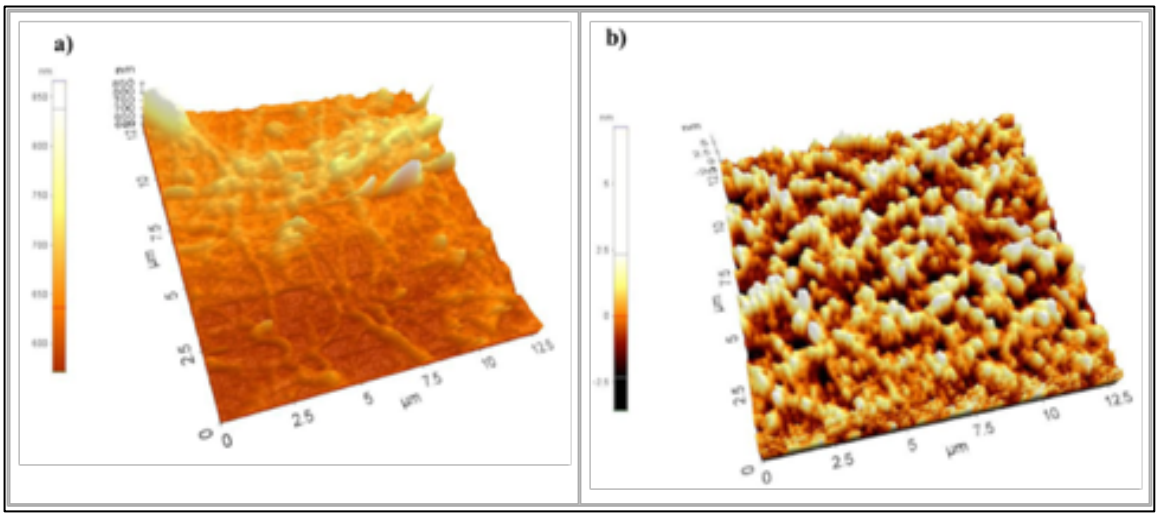

Figure 5.5. AFM Images of samples a) pretretated with solvent of 8% (w/v) LiCL-DMA for 2 days at room temperature and degraded with liquid nitrogen. b) pretretated with solvent of 8% (w/v) LiCL-DMA for 2 days at room temperature and treated with 40% sulphuric acid with autoclave for 15 min at 121°C.

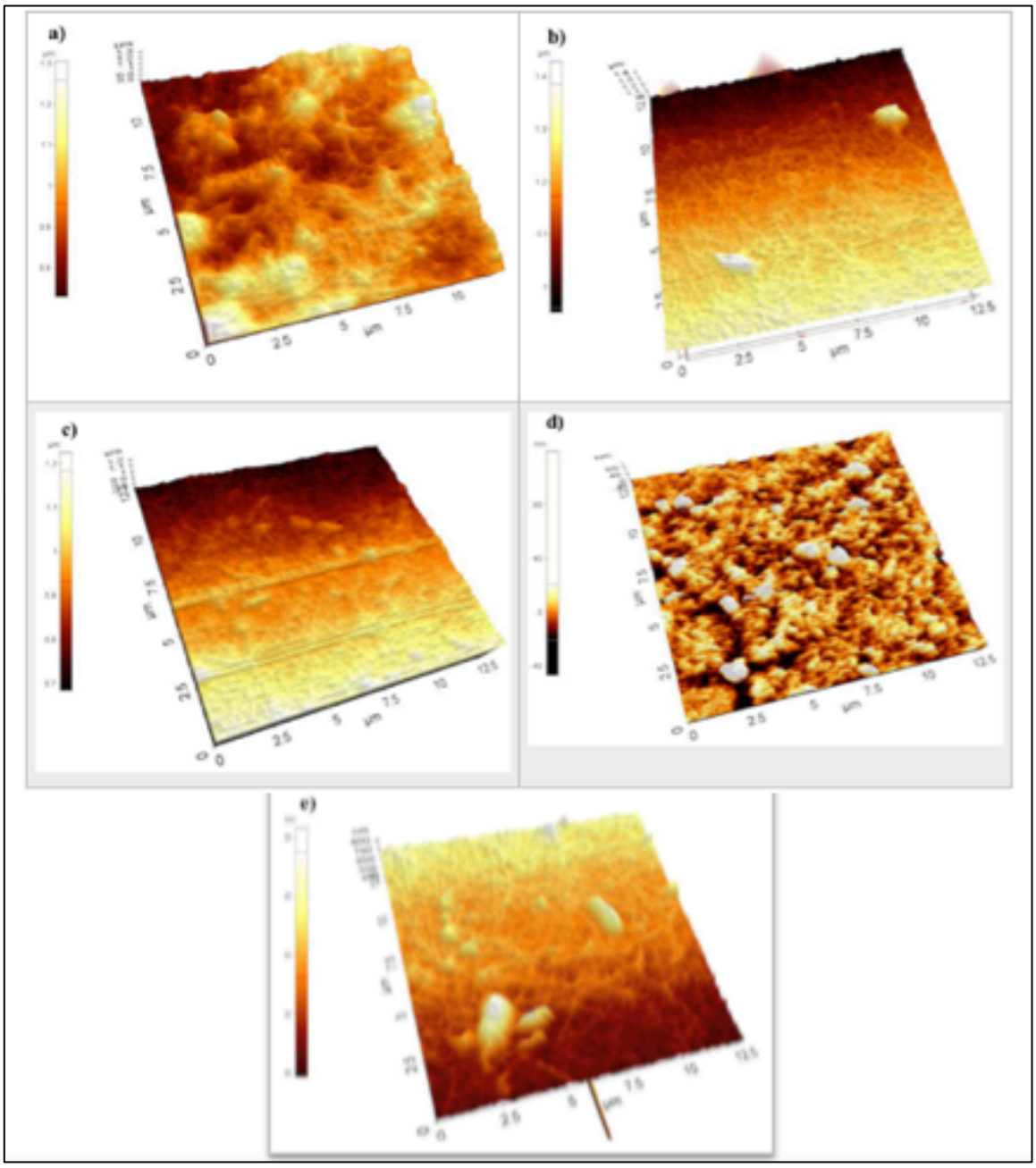

Figure 5.6. AFM Image of samples a) pretreated with 40% sulphuric acid with autoclave for 15 min at 121°C b) pretreated with 40% sulphuric acid with autoclave for 15 min at 121°C and degraded with 65% sulphuric acid at room temperature for 2 days c) pretreated with 40% sulphuric acid at room temperature for 1 hour 40 min and degraded with 65% sulphuric acid at room temperature for 2 days d) pretreated with 40% sulphuric acid with autoclave for 45 min at 121°C and degraded with 65% sulphuric acid at room temperature for 2 days e) pretreated with 40% sulphuric acid at room temperature for 2 hours 40 min and degraded with 65% sulphuric acid at room temperature for 2 days

Figure 5.6. demonstrated that the pretreatment of 40 percent sulphuric acid with an autoclave for 15 min indicated that bacterial cellulose network structure was preserved and aggregates can be observed for sample 6. When the degradation step with 65 percent sulphuric acid for 2 days was added, bacterial cellulose fibrils can be observed and clustered structures decreased for sample 16. Besides, with increasing time of the steam explosion the structure of bacterial cellulose was completely altered, and the network structure was broken, thereby sphere-like degraded nanocrystals were observed for sample 15. Additionally, samples exposed to acid at room temperature were close to each other in terms of network structure as can be seen in sample 4 and sample 9. However, the fibrillar structure in sample 4 is more observable than in sample 9.

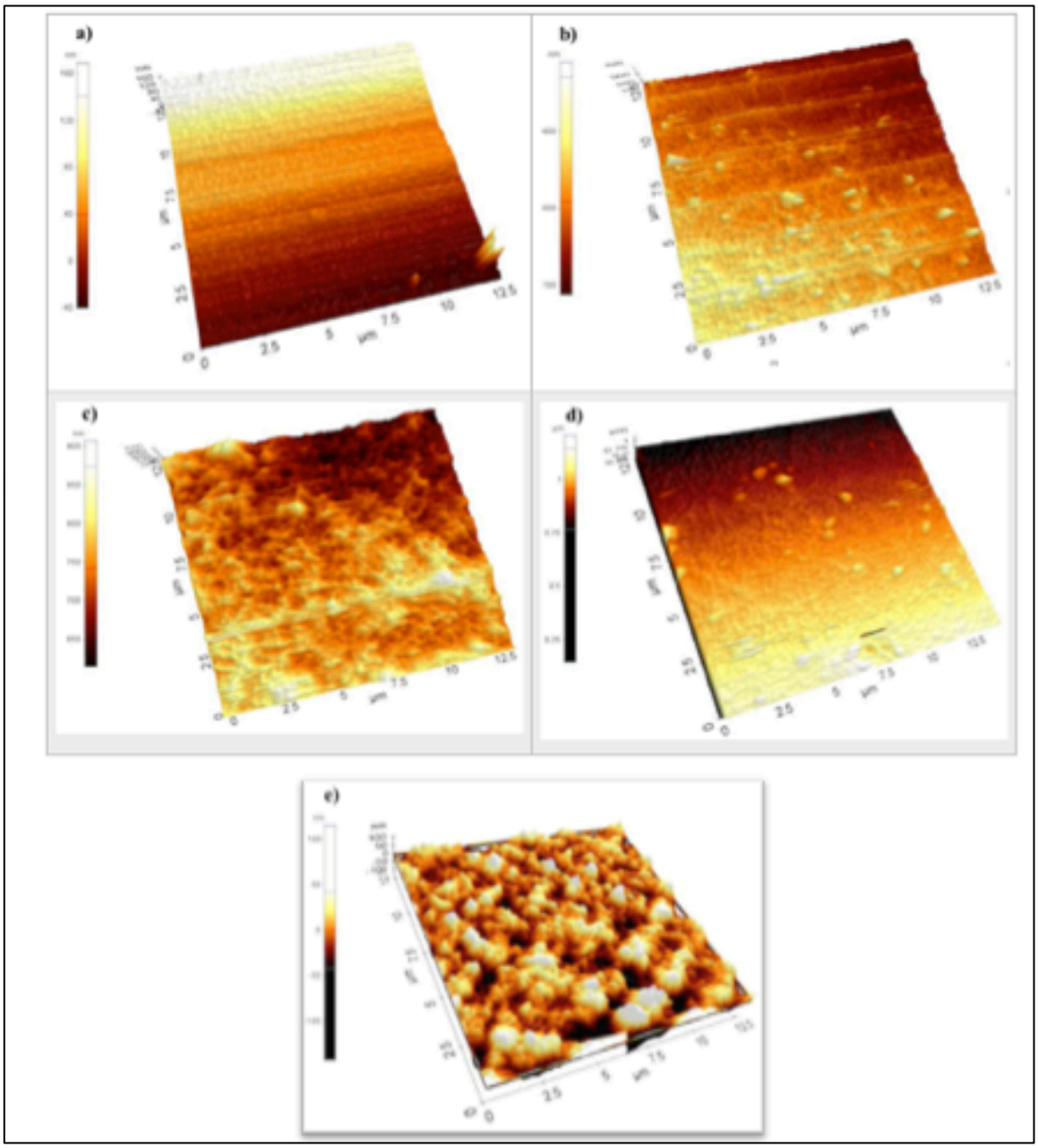

Figure 5.7. AFM Image of samples a) treated with 65% sulphuric acid at room temperature for 2 days b) pretreated with 65% sulphuric acid with autoclave for 15 min at 121°C and degraded with 65% sulphuric acid at room temperature for 2 days c) pretreated with 65% sulphuric acid at room temperature for 1 hour 40 min and degraded with 65% sulphuric acid at room temperature for 2 days d) pretreated with 65% sulphuric acid with autoclave for 45 min at 121°C and degraded with 65% sulphuric acid at room temperature for 2 days e) pretreated with 65% sulphuric acid at room temperature for 2 hours 40 min and degraded with 65% sulphuric acid at room temperature for 2 days

Sample 8 and sample 12, were different from each other. As mentioned above, when 65 percent sulphuric acid degradation was combined with autoclave pretreatment BC samples were broken into nanofibrils. Moreover, acid concentration increased degraded network structure was obtained. Furthermore, sphere-like degraded nanofibrils aggregates were observed for sample 7 in the Figure 5.7.

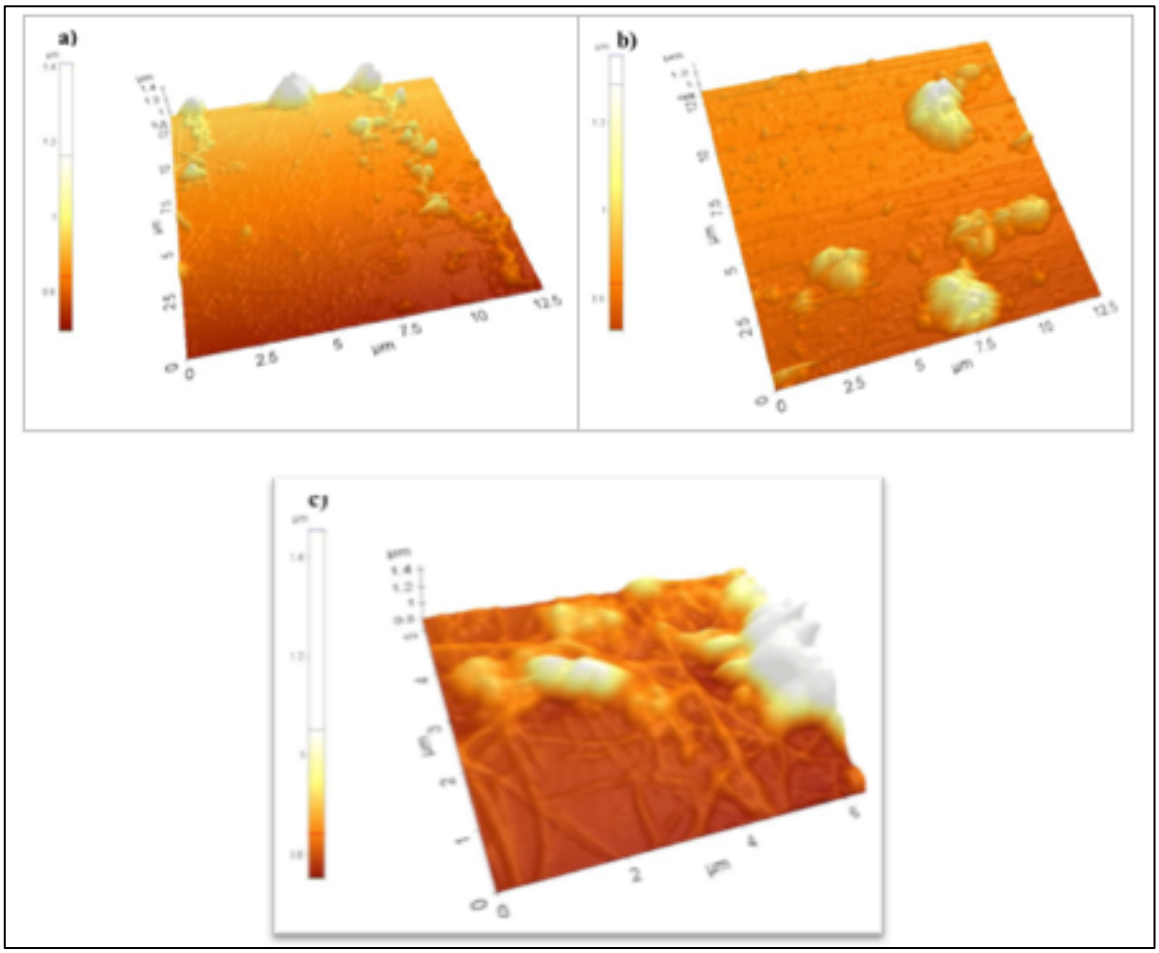

Figure 5.8. AFM Image of samples a) pretreated with 90% sulphuric acid with autoclave for 15 min at 121°C and degraded with 65% sulphuric acid at room temperature for 2 days b) pretreated with 90% sulphuric acid at room temperature for 1 hour 40 min and degraded with 65% sulphuric acid at room temperature for 2 days c) pretreated with 90% sulphuric acid at room temperature for 2 hours 40 min and degraded with 65% sulphuric acid at room temperature for 2 days

According to the 90 percent sulphuric acid pretreatment results, Figure 5.8c showed nanofibrils and aggregates clearly for sample 5. Also, sample 10 demonstrated nanocrystal

structures. However, in the Figure 5.8. sample 11 indicated small sphere-like structures like the other autoclave pretreatments.

5.4. FT-IR SPECTRUM ANALYSIS

FT-IR spectra of the samples were taken from 525 cm^{-1} to 4000 cm^{-1}. According to the Garside and Wyeth assignment of cellulose infrared bands as following.

Table 5.3. Infrared band assignments of cellulose [120]

Frequency (cm^{-1})	Assignment	Frequency (cm^{-1})	Assignment
~ 3340	3-OH···O-5	~ 1162	CH
~ 2900	CH_2	~ 1110	C-2···O-2
~ 1726	C=O	~ 1060	C-O-C
~ 1600	C=C	~ 1003	C-3···O-3
~ 1420	CH_2	~ 895	CH/COC
~ 1250	CH+COH	~ 650	RING

The obtained peaks between 525 cm^{-1} to 4000 cm^{-1} are listed below in Table 5.4. Also, FT-IR spectra of sample 1, sample 2, sample 3, sample 4, sample 5, sample 6, sample 7, sample 8, sample 9, sample 10, sample 11, sample 12, sample 13, sample 14, sample 15 and sample 16 are found respectively in Appendix B.

Table 5.4. Infrared bands for all samples

Samples	Infrared Bands (cm-1)
90% sulphuric acid pretreatment with autoclave for 45 min at 121 °C and degradation with 65% sulphuric acid at room temperature for 2 days	860, 1026, 1144, 1605, 1681, 2848, 2915, 3361.
65% sulphuric acid pretreatment with autoclave for 45 min at 121 °C and degradation with 65% sulphuric acid at room temperature for 2 days	860, 1029, 1106, 1157, 1683, 2846, 2892, 3336.
40% sulphuric acid pretreatment with autoclave for 45 min 121 °C and degradation with 65% sulphuric acid at room temperature for 2 days	885, 900-1172, 1613, 2888, 3338.
90% sulphuric acid pretreatment at room temperature for 2h 40m and degradation with 65% sulphuric acid at room temperature for 2 days	868, 1029, 1035, 1106, 1158, 1658, 2847, 2892, 3336.
65% sulphuric acid pretreatment at room temperature for 2h 40m and degradation with 65% sulphuric acid at room temperature for 2 days	864, 1029, 1034, 1104, 1158, 1657, 2886, 3339.
40% sulphuric acid pretreatment at room temperature for 2h 40m and degradation with 65% sulphuric acid at room temperature for 2 days	867, 981-1031, 1104, 1158, 2888, 3339.
90% sulphuric acid pretreatment with autoclave for 15 min at 121 °C and degradation with 65% sulphuric acid at room temperature for 2 days	855, 1026, 1103, 1152, 1677, 2846, 2914, 3334.
65% sulphuric acid pretreatment with autoclave for 15 min at 121 °C and degradation with 65% sulphuric acid at room temperature for 2 days	879, 1025, 1099, 1105, 1156, 1665, 2848, 2912, 3334.
40% sulphuric acid pretreatment with autoclave for 15 min at 121 °C and degradation with 65% sulphuric acid at room temperature for 2 days	870, 1024, 1102, 1157, 1310, 1420, 2888, 3334.
90% sulphuric acid pretreatment at room temperature for 1h 40m and degradation with 65% sulphuric acid at room temperature for 2 days	847, 1025-1652, 2327, 2849, 2917, 3316.

65% sulphuric acid pretreatment at room temperature for 1h 40m and degradation with 65% sulphuric acid at room temperature for 2 days	657, 862, 1029-1419, 1678, 2330, 2887, 3337.
40% sulphuric acid pretreatment at room temperature for 1h 40m and degradation with 65% sulphuric acid at room temperature for 2 days	657, 863, 1028-1421, 1680, 2885, 3336.
8% (w/v) LiCl-DMA pretreatment for 2 days at room temperature and degradation with Liquid Nitrogen	882, 1029, 1053, 1104, 1156, 1603, 2884, 3336.
8% (w/v) LiCl-DMA pretreatment for 2 days at room temperature and treated with 40% sulphuric acid with autoclave for 15 min at 121 °C	657, 869, 1029, 1026, 1104, 1158, 3338, 1172-1421, 1678, 2888.
65% sulphuric acid at room temperature for 2 days	656, 863, 1028, 1103, 1151, 1670, 2874, 3339.
40% sulphuric acid with autoclave for 15 min at 121 °C	658, 866, 1029-1420, 1668, 2888, 3339.

According to Figure 5.9 and Table 5.4., sample 2 had the sharp peaks were located at 657 cm^{-1}, 869 cm^{-1}, 1029 cm^{-1}, 1026 cm^{-1}, 1104 cm^{-1}, 1158 cm^{-1} and 3338 cm^{-1}; small peaks around 1172-1421 cm^{-1}, 1678 cm^{-1} and 2888 cm^{-1} whereas sample 8 had broaden peaks were located at 1670 cm^{-1}, 2874 cm^{-1}, 3339 cm^{-1} and sharper peaks were around 656 cm^{-1}, 863 cm^{-1}, 1028 cm^{-1}, 1103 cm^{-1}, 1151 cm^{-1}.

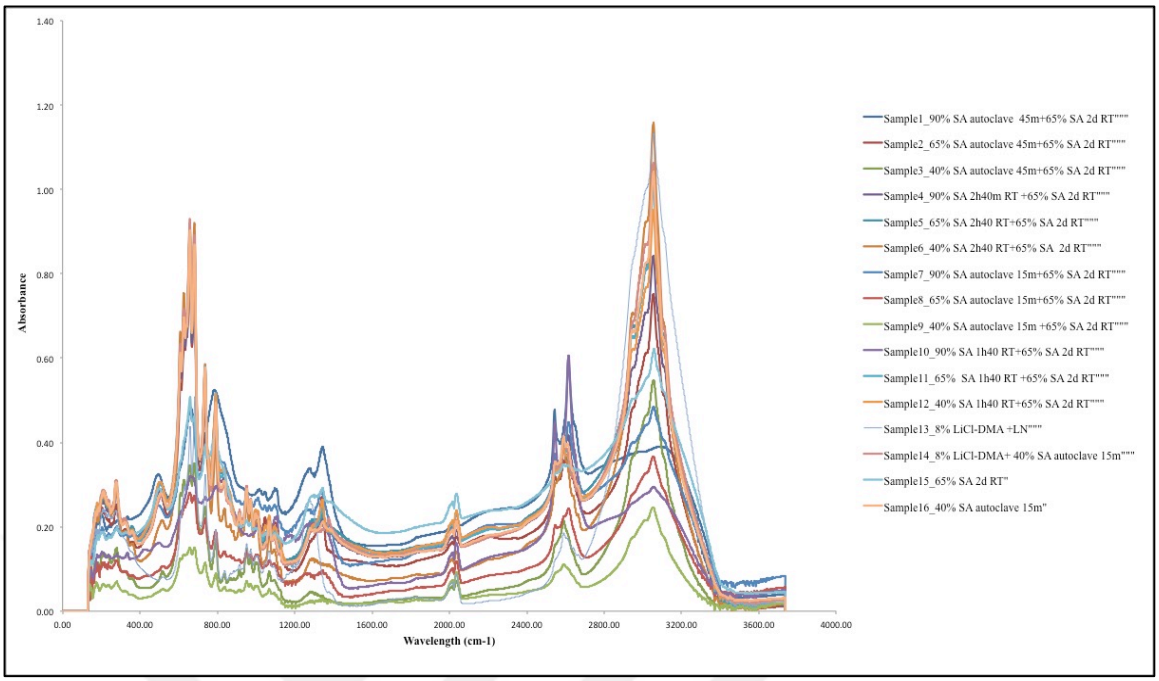

Figure 5.9. FT-IR spectra of the chemically degraded bacterial cellulose samples under different conditions

The bands at around 3340 cm^{-1} are related to the main hydrogen bonds for 3-OH···O5 according to Table 5.3. According to Figure 5.9., two samples are having broad bands around 3400 cm^{-1} as can be seen for sample 1 and sample 11. Also, at this point more intensive peaks refer to sample 4. and sample 1. On the other hand, cellulose vibration bands for sample 1, sample 9, and sample 11 shifted left. However, sample 3 shifted right which means the stretching of O-H bonds for bacterial cellulose nanocrystals.

The wavelength around 2900 cm^{-1} corresponds to C-H stretching vibration which is an obvious peak for all degraded BC samples in this study. There are only a few differences among them. For instance, sample 1 has less intensive peak than others, while sample 3, sample 10, and sample 11 have greater absorbance values. Moreover, sample 8 has broad one band around 2900 cm^{-1} whereas sample 13, and sample 12 have slightly broad two bands. In addition, sample 3, sample 5, sample 10, and sample 11 have narrow two peaks around this point.

Besides, the band around 870-900 cm^{-1} demonstrated characteristic bands of bacterial cellulose. All samples have this band with some differences. For instance, sample 10 and

sample 11 shifted left while sample 1 indicated a very small band around this interval. In this way, angular C-H bond deformation was observed except for sample 1.

On the other side, C-OH out of plane bending is related to 665-670 cm^{-1}. Several samples have weak intensity peaks which are shifted left from this interval such as sample 14, sample 9, sample 2, sample 8, and sample 6. The different degradation conditions cause C-OH bending.

The bands of absorption spectra through 1200 cm^{-1}-1000 cm^{-1} indicate that units have inter- and intramolecular bonding. For instance, sample 3 has two bands around due to CH_2 symmetric bending and C-C stretching. Sample 12 showed that C-C-OH bonds stretching, C-C stretching, and symmetrical stretching of C-O-C glycoside bonds. Also, Sample 15 indicated C-C stretching. All samples have various stretchings and bendings at 1000-1200 cm^{-1}. Nevertheless, 90 percent sulphuric acid pretreatment with autoclave for 45 min has more absorbance values than others. Moreover, 40 percent sulphuric acid pretreatment with autoclave for 15 min and 45 min are close to each other. Last but not least, solvent treatment with 8 percent LiCl-DMA and degradation with liquid nitrogen has weaker bands than autoclave pretreatments and acid treatments at room temperature.

5.5. DSC RESULTS

The first endothermic peak for sample 4 (40 percent sulphuric acid treatment for 2 hours 40 min) was at 63.46 °C, and the second endothermic peak was at 161.4 °C. Also, the first endothermic peak for sample 8 (65 percent sulphuric acid treatment at room temperature for 2 days) which is the main degradation process was at 50.03 °C, and the second peak at 156.91 °C. Sample 3 (90 percent sulphuric acid pretreatment with autoclave 45 min and degradation with 65 percent sulphuric acid at room temperature for 2 days) had shifted the first endothermic peak around 102.92 °C and the second peak was also shifted to 225.4 °C. The temperature of 146.41 °C referred to the first endothermic peak of sample 1 which was exposed to 8 percent LiCl-DMA and degraded with liquid nitrogen as can be seen Figure 5.10.

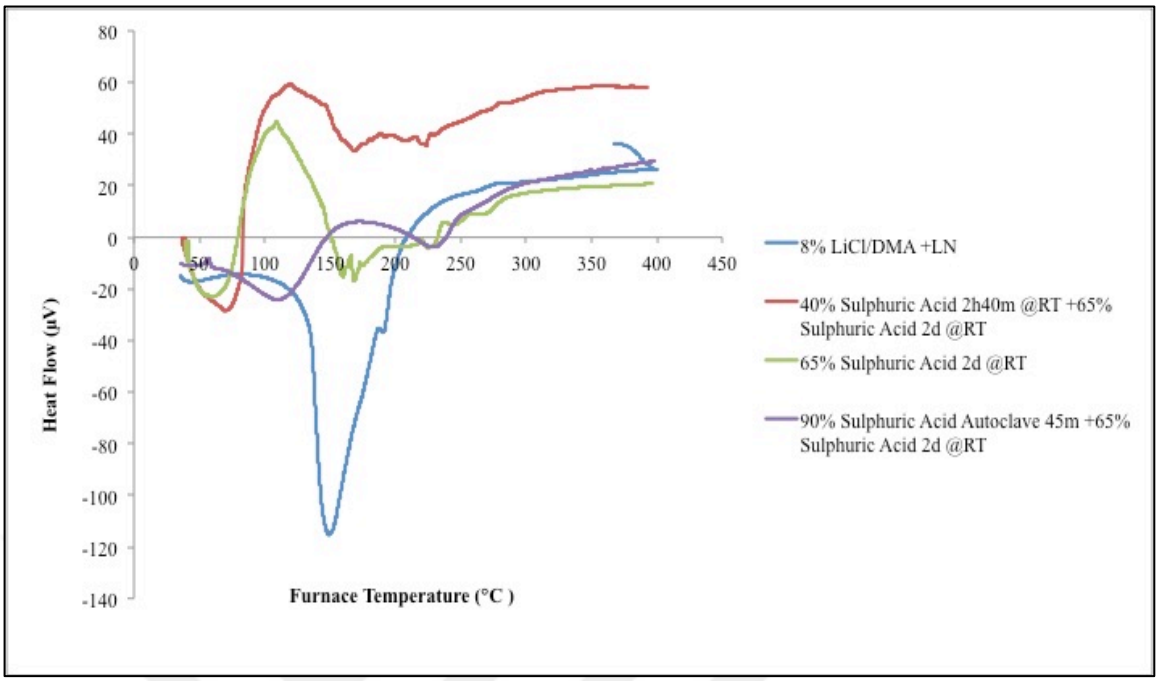

Figure 5.10. Differential scanning calorimetry curve of degraded bacterial cellulose samples

6. DISCUSSION

The purpose of the study is the chemical degradation of BC pellicle produced by *Gluconacetobacter xylinus* under different conditions and characterized by several methods. Bacterial cellulose is a widely used material having distinct properties and it has various applications, especially medical area and industry. Based on its ability to degrade, different degradation processes and characterizations are considered in this study. As a result, the different pretreatments led to different nanocellulose structures which can be used in various applications in the biomedical area. In the process of acid degradation, hydronium ions can attack the amorphous region of the glycosidic bond and release crystalline regions. Addition to that, sulphuric acid causes the esterification of anionic sulfate ester groups with surface hydroxyl groups. Therefore, samples can disperse in water due to the fact that the surface of the samples has a negative electrostatic layer [121].

The images after the degradation process of samples can be seen in Appendix A. Initially, the degraded samples had distinct features in terms of appearance. For instance, Figure A.2. sample 10, sample 11, sample 3, and sample 5 had black and ball-like degraded samples whereas, Figure A.3. sample 12, sample 7, sample 13, and sample 14 had viscous samples. It is stated that when hydrolysis temperature increases (higher than 60 °C) darkening of cellulose particles can be observed due to the carbonization and hydration [122]. The high acid concentration and high temperature can cause the darkening of the particles. In addition to that, autoclave pretreated samples such as sample 12, and sample 13 had smooth textures. In contrast, sample 7 and sample 14 which were room temperature pretreated for the total autoclave period were fragmented. Moreover, Figure A.4. included sample 15, sample 4, sample 16, and sample 9 were similar to Figure A.3. in the manner of appearance. However, Figure A.5. sample 1 and sample 2 had more fragmented structures when it was compared to others. Furthermore, more clustered structures were observed for sample 2 rather than sample 1. Consequently, various degradation conditions changed bacterial cellulose pellicle structures in different ways.

The morphology of degraded bacterial cellulose samples was observed with the help of SEM and TEM. It is stated that bacterial cellulose pellicle is made of rod-shaped nanofibers ranging from 50 nm to 70 nm and it has an ultrafine network structure that is held together via hydrogen bonding. Also, nanofibers have a 67.5 ± 9.4 nm diameter.

However, BC nanocrystals have an average diameter of 20-30 nm [105]. Addition to that, it is revealed that sulphuric acid hydrolysis creates rod-like cellulose nanocrystals with negatively charged surface acid groups of $OSO3^{-}/H^{+}$[123]. According to SEM images of two different conditions, 65 percent sulphuric acid pretreatment with autoclave for 45 min caused degradation of bacterial cellulose ultrafine network structure and generation BC nanostructures. Roman et. al indicated that the length of degraded bacterial cellulose fragments varies from 200 nm to several micrometers [124]. Besides, Yan et al. demonstrated that hydrolyzed crystalline microfibrils have a diameter between 8-40 nm. With the cleavage of amorphous components, rod-like and short microfibrils are constituted [103]. Moreover, George et. al stated that 65 percent sulphuric acid treatment for 3h provided the nanocrystals with a length of 100-300 nm and width of 10-20 nm [125]. Regarding a rough estimation of TEM results, bacterial cellulose nanofibrils and nanocrystals are ranging from 300 nm to 700 nm in size with widths from 9 nm to 18 nm when the results are compared to Figure 5.3. Furthermore, there are sphere-like bacterial nanocrystals could be obtained with the combination of solvent pretreatment and acid with autoclave treatment. Since Neng et. al revealed that spherical cellulose nanocrystals are able to be obtained with the help of mixed acid concentration at proper ratio and ultrasonication. The principle is that acid can easily penetrate the inner amorphous region by using ultrasonication. In this way, a hydrolysis reaction can occur at the surface of the amorphous region and inner region at the same time [97]. In this study, solvent pretreatment and acid treatment with autoclave could provide the penetration of acid to the inner amorphous region.

Moreover, Chirayil et. al demonstrated that steam explosion with acid treatment provides both individual nanofibrils and some aggregates. It is expected that the treatment of acid cleaves the amorphous region of the microfibrils and reduces the fiber size [113]. Therefore, when TEM results are considered, the size of the sample exposed to 40 percent sulphuric acid pretreatment with autoclave is reduced than 40 percent sulphuric acid pretreatment at room temperature. Additionally, the increasing acid concentration led to a smaller length of particles. On the other side, when sample 4 and sample 6 are considered, autoclave pretreatment also reduces the width of the sample. This result is matched with FT-IR results in terms of hydrogen bonding (OH stretching bands) interruption.

The dissolution of bacterial cellulose in 8 percent LiCl-DMA results in the disappearance of the fibrillar structure of BC. The transparent bacterial cellulose pellicle is obtained in this way. That ensures the transformation of the crystalline state to the amorphous structure [118]. It is expected that liquid nitrogen degradation which is the grinding process for acquiring cellulose nanofibers [126] has a higher average size in length.

According to AFM results, there are nanofibers, nanocrystals, and spherical nanocrystals structures as can be seen in Figure 5.5., Figure 5.6., Figure 5.7. and Figure 5.8. Also, there are some aggregates in these figures. It is expected that sulphuric acid treatment results in nanocrystal formation and grinding causes the nanofibers formation [119]. According to Chirayil et. al AFM images of cellulose nanofibrils [113] are similar with 40 percent sulphuric acid pretreatment with autoclave 15 min and 40 percent sulphuric acid pretreatment with autoclave and degradation with 65 percent sulphuric acid at room temperature for 2 days. Also, solvent pretreatment with liquid nitrogen degradation is very distinct from solvent pretreatment with autoclave treatment. Moreover, with the help of 65 percent sulphuric acid treatment, rod-like nanocrystal structures can be obtained as stated above, with the increasing reaction time nanofibrils can be converted to nanocrystals. Therefore nanocrystals and nanofibers can be seen in AFM results. TEM results support the AFM images. On the other hand, AFM images also included some aggregates. This is raised by strong hydrogen bonding between the fibrils [113]. According to the TEM and AFM results, the sample is pretreated with 90 percent sulphuric acid with autoclave 45 min and degraded with 65 percent sulphuric acid at room temperature for 2 days, TEM and AFM images could not be obtained due to harsh degradation conditions, however, FT-IR spectrum of this sample was acquired and cellulose vibration peak shifted right. As a result of TEM and AFM images, nanofiber structures were obtained except for sample 2, and sample 10, since they were spherical nanocrystals.

FT-IR spectra are used for obtaining information on chemical changes which are generated during the degradation of bacterial cellulose samples. The various changes in the sample composition were observed. According to FT-IR analysis, it is stated that 3338.41 cm^{-1} corresponds to -OH stretching and 2917.85 cm^{-1} is for –C-H stretching. It can be understood that with the narrow peaks hydrogen bonding between fibrils is preserved. When bands are broad, it is considered that hydrogen bonding between fibrils is disturbed and degradation occurs. This result match with TEM images. For instance, the width of

sample 4 is greater than sample 6 due to the hydrogen bonding. Besides, the pretreatment of autoclave and high concentration acid led to more degradation of bacterial cellulose, whereas low concentration acid and room temperature pretreatment ensure retaining the inter and intramolecular hydrogen bonding. When autoclave pretreatment for 45 min results are compared, OH stretching band is dramatically changed for sample 3. It indicated that intramolecular hydrogen bonding is more damaged than sample 12 and sample 15. Also, 1015.65 cm^{-1} is associated with the stretching of C-C, C-OH, C-H ring, and C-O-C at the β-(1→4)-glycosidic bond [90]. Furthermore, 1056 cm^{-1} is related to bacterial cellulose vibration of C-O-C stretching. At around 3340 cm^{-1} bands is due to the 3-OH···O-5 hydrogen bond while 2900 cm^{-1} bands are assigned to the CH_2. The C-H stretching bands are higher in autoclave pretreatment than room temperature pretreatment and solvent pretreatment. This could be originated in the process of cellulose degradation. Firstly, hydronium ions penetrate the glycosidic bond and it is disturbed. After that, water molecules attack the carbon atom. At this point, C-H stretching and C-OH bending and H-C-H bending can occur. However, peaks through 1000-1200 cm^{-1} result from H-C-H and C-OH bending, indicating inter- and intramolecular linkage of the units [127]. On the other hand, Fittipaldi et. al stated that 897 cm^{-1} is linked with C-H bond deformation, 1163 cm^{-1} is for C-O-C glycoside bond stretching, and 1371 cm^{-1} is named as C-H bond of symmetric angular deformation and lastly, 1429 cm^{-1} is connected with the C-H bond of asymmetric angular deformation. Also, they indicated that 807 cm^{-1} is linked with the C-O-S vibration [102]. In this study, there were bands through 1000-1200 cm^{-1}, around 2900 cm^{-1}, around 3340 cm^{-1}, and also around 870-900 cm^{-1}. Additionally, there were 665-670 cm^{-1} peaks. It means that 665-670 cm^{-1} causes C-OH bending. In other respects, there were no 807 cm^{-1} bands that are related to C-O-S vibration. It means that esterification did not occur during the hydrolysis reaction.

The DSC results are considered, Fittipaldi et. al revealed that the endothermic peak at 136.7 °C is the crystalline melting point (T_m) of the bacterial cellulose. Similarly, after the exothermic peak at 350.72 °C, degradation is occurred (T_m). Addition to that, the endothermic peak of BCNCs is between 140-195 °C, especially 60-65 percent sulphuric acid treated samples give peaks in the range of 200-290 °C [102]. Sample 4 and sample 8 are close to each other in terms of T_c (crystalline temperature) and T_m (melting temperature). However, sample 3 and sample 1 had larger T_c and T_m than sample 4 and

sample 8. It can be understood that high concentration acid with autoclave pretreatment and solvent pretreatment with mechanical degradation caused more structural changes. These results are also supported by the TEM and FT-IR spectra of these samples.

7. CONCLUSION

In conclusion, the different chemical treatment and pretreatment procedures were applied to bacterial cellulose pellicle which is produced by *Gluconacetobacter xylinus* FC01 strain using the defined medium as M1A05P5. The changes in the morphology are analyzed using SEM, AFM, and TEM. SEM results indicated the nanofibril structures for acid pretreatment with autoclave. AFM results showed both nanocrystals which resulted from 90 percent acid pretreatment with autoclave and solvent pretreatment and the nanofibril structures that are obtained by acid treatments both autoclave and room temperature pretreatments. Also, the average length and width of degraded samples are estimated with the help of TEM images as 312.12-700 nm and 9.09-27.27 nm. The chemical changes in the structures are analyzed by FT-IR and DSC. The dramatic change in OH stretching in autoclave pretreatment steps is oberved by FT-IR spectra whereas T_c and T_m changes in solvent pretreatment and autoclave pretreatment are acquired by DSC. As a result, the bacterial cellulose samples are degraded into bacterial nanocrystals (BCNCs) with autoclave pretreatment for 90 percent acid, nanofibrils (BCNFs) with acid pretreatments for 65 percent, and 40 percent acid and spherical cellulose nanocrystals (SCNCs) with solvent pretreatment and autoclave treatment with 40 percent acid.

REFERENCES

1. Isik M, Sardon H, Mecerreyes D. Ionic liquids and cellulose: Dissolution, chemical modification and preparation of new cellulosic materials. *Int J Mol Sci.* 2014;15(7):11922–40.

2. Mélida H, Sandoval-Sierra J V., Diéguez-Uribeondo J, Bulone V. Analyses of extracellular carbohydrates in oomycetes unveil the existence of three different cell wall types. *Eukaryot Cell*. 2013;12(2):194–203.

3. Kögel-Knabner I, Amelung W. Dynamics, Chemistry, and Preservation of Organic Matter in Soils., *Treatise on Geochemistry*. 2013;12(2):157–215.

4. Sun S, Sun S, Cao X, Sun R. The role of pretreatment in improving the enzymatic hydrolysis of lignocellulosic materials. *Bioresour Technol*. 2016;199:49–58.

5. Moon RJ, Martini A, Nairn J, Simonsen J, Youngblood J. Cellulose nanomaterials review: Structure, properties and nanocomposites. *Chemical Society Reviews*. 2011; 40(7): 3941–3994.

6. John MJ, Thomas S. Biofibres and biocomposites. *Carbohydr Polym*. 2008;71(3):343–64.

7. Strachan J. Solubility of cellulose in water. *Nature*. 1938;141(3564):332–3.

8. O'Connell DW, Birkinshaw C, O'Dwyer TF. Heavy metal adsorbents prepared from the modification of cellulose: A review. *Bioresour Technol*. 2008;99(15):6709–24.

9. L.M.J. Kroon-Batenburg, J. Kroon, The crystal and molecular structures of cellulose I and II. *Glycoconjugate Journal*.1997;14:677-690.

10. Erdtmann M, Keller R, Baumann H. Photochemical immobilization of heparin, dermatan sulphate, dextran sulphate and endothelial cell surface heparan sulphate onto cellulose membranes for the preparation of athrombogenic and antithrombogenic polymers. *Biomaterials*. 1994;15(13):1043–8.

11. Ergun R, Guo J, Huebner-Keese B. Cellulose. *Encycl Food Heal*. 2015;694–702.

12. Poletto M, Pistor V, J. A. Structural Characteristics and Thermal Properties of Native Cellulose. *Cellulose Fundam Asp*. 2013:45-68.

13. Achwal WB, Chaugule DA. Investigations in modified alkaline iron-tartrate complex solvent for cellulose. *Die Angew Makromol Chemie*. 1975;42(1):77–89.

14. Klemm D, Heublein B, Fink HP, Bohn A. Cellulose: Fascinating biopolymer and sustainable raw material. A*ngew Chemie - Int Ed*. 2005;44(22):3358–93.

15. U.S. Congress, Office of Technology Assessment, Technologies for Reducing Dioxin in the Manufacture of Bleached Wood Pulp. 1989.

16. Processes P. Chapter 6: Pulp and paper. *Regul Toxicol Pharmacol*. 1994;20(1):S308–415.

17. Casaburi A, Montoya Rojo Ú, Cerrutti P, Vázquez A, Foresti ML. Carboxymethyl cellulose with tailored degree of substitution obtained from bacterial cellulose. *Food Hydrocoll*. 2018;75:147–56.

18. Capitani D, Del Nobile MA, Mensitieri G, Sannino A, Segre AL. 13C solid-state NMR determination of cross-linking degree in superabsorbing cellulose-based networks. *Macromolecules*. 2000;33(2):430–7.

19. Blachechen LS, Amim J, Lincopan N, Petri DFS. Carboxymethylcellulose acetate butyrate/poly(4-vinyl-N-pentyl pyridinium bromide) blends as antimicrobial coatings. *Express Polym Lett*. 2015;9(9):790–8.

20. Pathak PD, Mandavgane SA, Kulkarni BD. Fruit peel waste as a novel low-cost bio adsorbent. *Rev Chem Eng*. 2015;31(4):361–81.

21. Carter EA, Swarbrick B, Harrison TM, Ronai L. Rapid identification of cellulose nitrate and cellulose acetate film in historic photograph collections. *Heritage Sci.* 2020;8(1):1–13.

22. Reis DT, Pereira AKDS, Scheidt GN, Pereira DH. Plant and bacterial cellulose: Production, chemical structure, derivatives and applications. *Orbital*. 2019;11(5):321–9.

23. Ul-Islam M, Khan S, Ullah MW, Park JK. Comparative study of plant and bacterial cellulose pellicles regenerated from dissolved states. I*nt J Biol Macromol*. 2019;137:247–52.

24. Ullah MW, Ul-Islam M, Khan S, Kim Y, Park JK. Structural and physico-mechanical characterization of bio-cellulose produced by a cell-free system. *Carbohydr Polym.* 2016;136:908–16.

25. Khalid A, Khan R, Ul-Islam M, Khan T, Wahid F. Bacterial cellulose-zinc oxide nanocomposites as a novel dressing system for burn wounds. *Carbohydr Polym.* 2017;164:214–21.

26. Naomi R, Idrus RBH, Fauzi MB. Plant-vs. Bacterial-derived cellulose for wound healing: A review. *Int J Environ Res Public Health*. 2020;17(18):1–25.

27. Fu L, Zhang J, Yang G. Present status and applications of bacterial cellulose-based materials for skin tissue repair. *Carbohydr Polym*. 2013;92(2):1432–42.

28. Khan S, Ul-Islam M, Ikram M, Ullah MW, Israr M, Subhan F, et al. Three-dimensionally microporous and highly biocompatible bacterial cellulose-gelatin composite scaffolds for tissue engineering applications. *RSC Adv.* 2016;6(112):110840–9.

29. Cannon RE, Anderson SM. Biogenesis of bacterial cellulose. *Crit Rev Microbiol.* 1991;17(6):435–47.

30. Jonas R, Farah LF. Production and application of microbial cellulose. *Polym Degrad Stab*. 1998;59(1–3):101–6.

31. Lee JW, Deng F, Yeomans WG, Allen AL, Gross RA, Kaplan DL. Direct Incorporation of Glucosamine and N-Acetylglucosamine into Exopolymers by Gluconacetobacter xylinus (=Acetobacter xylinum) ATCC 10245: Production of Chitosan-Cellulose and Chitin-Cellulose Exopolymers. *Appl Environ Microbiol.* 2001;67(9):3970–5.

32. Liu M, Liu L, Jia S, Li S, Zou Y, Zhong C. Complete genome analysis of Gluconacetobacter xylinus CGMCC 2955 for elucidating bacterial cellulose

biosynthesis and metabolic regulation. *Sci Rep*. 2018;8(1):1–10.

33. Fontana JD, De Souza AM, Fontana CK, Torriani IL, Moreschi JC, Gallotti BJ, et al. Acetobacter cellulose pellicle as a temporary skin substitute. *Appl Biochem Biotechnol.* 1990;24–25(1):253–64.

34. Embuscado ME, Marks JS, BeMiller JN. Bacterial cellulose. I. Factors affecting the production of cellulose by Acetobacter xylinum. *Top Catal*. 1994;8(5):407–18.

35. Scott Williams WS, Cannon RE. Alternative environmental roles for cellulose produced by Acetobacter xylinum. *Appl Environ Microbiol.* 1989;55(10):2448–52.

36. Chawla PR, Bajaj IB, Survase SA, Singhal RS. Microbial cellulose: Fermentative production and applications. *Food Technol Biotechnol.* 2009;47(2):107–24.

37. Festucci-Buselli RA, Otoni WC, Joshi CP. Structure, organization, and functions of cellulose synthase complexes in higher plants. *Brazilian J Plant Physiol.* 2007;19(1):1–13.

38. Costa AFS, Almeida FCG, Vinhas GM, Sarubbo LA. Production of bacterial cellulose by Gluconacetobacter hansenii using corn steep liquor as nutrient sources. *Front Microbiol.* 2017;8:1–12.

39. Lee HC, Zhao X. Effects of mixing conditions on the production of microbial cellulose by Acetobacter xylinum. *Biotechnol Bioprocess Eng.* 1999;4(1):41–5.

40. Mohite B V., Patil S V. Investigation of Bacterial Cellulose Biosynthesis Mechanism in Gluconoacetobacter hansenii . *International Scholarly Research Notices*. 2014;2014:1–7.

41. Richards et al. 乳鼠心肌提取 HHS Public Access. *Physiol Behav.* 2018;176(5):139–48.

42. Lee KY, Buldum G, Mantalaris A, Bismarck A. More than meets the eye in bacterial cellulose: Biosynthesis, bioprocessing, and applications in advanced fiber composites. *Macromol Biosci.* 2014;14(1):10–32.

43. Glaser L. The enzymic synthesis of cellulose by Acetobacter xylinum. BBA - *Biochim Biophys Acta.* 1957;25(2):436.

44. Omadjela O, Narahari A, Strumillo J, Mélida H, Mazur O, Bulone V, et al. BcsA and BcsB form the catalytically active core of bacterial cellulose synthase sufficient for in vitro cellulose synthesis. P*roc Natl Acad Sci U S A.* 2013;110(44):17856–61.

45. Wong HC, Fear AL, Calhoon RD, Eichinger GH, Mayer R, Amikam D, et al. Genetic organization of the cellulose synthase operon in Acetobacter xylinum. *Proc Natl Acad Sci U S A.* 1990;87(20):8130–4.

46. Standal R, Iversen TG, Coucheron DH, Fjaervik E, Blatny JM, Valla S. Erratum: A new gene required for cellulose production and a gene encoding cellulolytic activity in Acetobacter xylinum are colocalized with the bcs operon. *J Bacteriol.* 1994;176(11):3443.

47. Deng Y, Nagachar N, Xiao C, Tien M, Kao TH. Identification and characterization of non-cellulose-producing mutants of Gluconacetobacter hansenii generated by Tn5 transposon mutagenesis. *J Bacteriol.* 2013;195(22):5072–83.

48. Sunagawa N, Fujiwara T, Yoda T, Kawano S, Satoh Y, Yao M, et al. Cellulose complementing factor (Ccp) is a new member of the cellulose synthase complex (terminal complex) in Acetobacter xylinum. *J Biosci Bioeng.* 2013;115(6):607–12.

49. Umeda Y, Hirano A, Ishibashi M, Akiyama H, Onizuka T, Ikeuchi M, et al. Cloning of cellulose synthase genes from Acetobacter xylinum JCM 7664: Implication of a novel set of cellulose synthase genes. *DNA Res.* 1999;6(2):109–15.

50. Römling U, Galperin MY. Bacterial cellulose biosynthesis: Diversity of operons, subunits, products, and functions. *Trends Microbiol.* 2015;23(9):545–57.

51. Masaoka S, Ohe T, Sakota N. Production of cellulose from glucose by Acetobacter xylinum. *J Ferment Bioeng*. 1993;75(1):18–22.

52. Hestrin S, Schramm M. Synthesis of cellulose by Acetobacter xylinum. II. Preparation of freeze-dried cells capable of polymerizing glucose to cellulose. *Biochem J.* 1954;58(2):345–52.

53. Matsuoka M, Tsuchida T, Matsushita K, Adachi O, Yoshinaga F. A Synthetic Medium for Bacterial Cellulose Production by Acetobacter xylinum subsp. sucrofermentans. *Biosci Biotechnol Biochem.* 1996;60(4):575–9.

54. Hussain Z, Sajjad W, Khan T, Wahid F. Production of bacterial cellulose from industrial wastes: a review. *Cellulose.* 2019;26(5):2895–911.

55. Revin V, Liyaskina E, Nazarkina M, Bogatyreva A, Shchankin M. Cost-effective production of bacterial cellulose using acidic food industry by-products. *Brazilian J Microbiol.* 2018;49:151–9.

56. Castro C, Zuluaga R, Putaux JL, Caro G, Mondragon I, Gañán P. Structural characterization of bacterial cellulose produced by Gluconacetobacter swingsii sp. from Colombian agroindustrial wastes. *Carbohydr Polym.* 2011;84(1):96–102.

57. Wang J, Tavakoli J, Tang Y. Bacterial cellulose production, properties and applications with different culture methods – A review. *Carbohydr Polym.* 2019;219:63–76.

58. Gao H, Sun Q, Han Z, Li J, Liao B, Hu L, et al. Comparison of bacterial nanocellulose produced by different strains under static and agitated culture conditions. *Carbohydr Polym*. 2020;227:115323.

59. Hsieh JT, Wang MJ, Lai JT, Liu HS. A novel static cultivation of bacterial cellulose production by intermittent feeding strategy. J *Taiwan Inst Chem Eng*. 2016;63:46–51.

60. Krystynowicz A, Czaja W, Wiktorowska-Jezierska A, Gonçalves-Miśkiewicz M, Turkiewicz M, Bielecki S. Factors affecting the yield and properties of bacterial cellulose. *J Ind Microbiol Biotechnol.* 2002;29(4):189–95.

61. Hu Y, Catchmark M, Vogler EA. Factors Impacting the Formation of Sphere-Like Bacterial Cellulose Particles and Their Biocompatibility for Human Osteoblast Growth. *Biomacromolecules.* 2013; 14(10):3444-52.

62. Andriani D, Apriyana AY, Karina M. The optimization of bacterial cellulose production and its applications: a review. *Cellulose.* 2020;27(12):6747–66.

63. Keshk SM. Bacterial Cellulose Production and its Industrial Applications. *J Bioprocess Biotech.* 2014;04(02):1-10.

64. Campano C, Balea A, Blanco A, Negro C. Enhancement of the fermentation process and properties of bacterial cellulose: a review. *Cellulose.* 2016;23(1):57–91.

65. Huang Y, Zhu C, Yang J, Nie Y, Chen C, Sun D. Recent advances in bacterial cellulose. *Cellulose.* 2014;21(1):1–30.

66. Qualities N. Quality Characteristics of Chinese-style Meatball Containing Bacterial Cellulose (Nata) Sensory and Nutritive Qualities of Food. *J Food Sci.* 2004;69(3).

67. Guo Y, Zhang X, Hao W, Xie Y, Chen L, Li Z, et al. Nano-bacterial cellulose/soy protein isolate complex gel as fat substitutes in ice cream model. *Carbohydr Polym*. 2018;198:620–30.

68. Tomé LC, Brandão L, Mendes AM, Silvestre AJD, Neto CP, Gandini A, et al. Preparation and characterization of bacterial cellulose membranes with tailored surface and barrier properties. *Cellulose.* 2010;17(6):1203–11.

69. da Silva CJG, de Medeiros ADM, de Amorim JDP, do Nascimento HA, Converti A, Costa AFS, et al. Bacterial cellulose biotextiles for the future of sustainable fashion: a review. *Environ Chem Lett.* 2021;19(4):2967–80.

70. Fernandes M, Souto AP, Dourado F, Gama M. Application of Bacterial Cellulose in the Textile and Shoe Industry: Development of Biocomposites. *Polysaccharides.* 2021;2(3):566–81.

71. Gregory DA, Tripathi L, Fricker ATR, Asare E, Orlando I, Raghavendran V, et al. Bacterial cellulose: A smart biomaterial with diverse applications. *Mater Sci Eng R Reports*. 2021;145:100623.

72. Pandit A, Kumar R. A Review on Production, Characterization and Application of Bacterial Cellulose and Its Biocomposites. *J Polym Environ*. 2021;29(9):2738–55.

73. Cacicedo ML, Castro MC, Servetas I, Bosnea L, Boura K, Tsafrakidou P, et al. Bioresource Technology Progress in bacterial cellulose matrices for biotechnological

applications. *Bioresour Technol.* 2016;213:172-180.

74. Abeer MM, Mohd Amin MCI, Martin C. A review of bacterial cellulose-based drug delivery systems: Their biochemistry, current approaches and future prospects. *J Pharm Pharmacol.* 2014;66(8):1047–61.

75. Silva NHCS, Rodrigues AF, Almeida IF, Costa PC, Rosado C, Neto CP, et al. Bacterial cellulose membranes as transdermal delivery systems for diclofenac: In vitro dissolution and permeation studies. *Carbohydr Polym*. 2014;106(1):264–9.

76. Badshah M, Ullah H, Khan AR, Khan S, Park JK, Khan T. Surface modification and evaluation of bacterial cellulose for drug delivery. *International Journal of Biological Macromolecules.* 2018;113:526–533.

77. Zhang LK, Du S, Wang X, Jiao Y, Yin L, Zhang Y, et al. Bacterial cellulose based composites enhanced transdermal drug targeting for breast cancer treatment. *Chem Eng J* . 2019;370:749–59.

78. Swingler S, Gupta A, Gibson H, Kowalczuk M, Heaselgrave W, Radecka I. Recent advances and applications of bacterial cellulose in biomedicine. *Polymers (Basel).* 2021;13(3):1–29.

79. Roman M, Haring AP, Bertucio TJ. The growing merits and dwindling limitations of bacterial cellulose-based tissue engineering scaffolds. *Curr Opin Chem Eng*. 2019;24:98–106.

80. Friedman SL. Extracellular matrix.*Signaling Pathways in Liver Diseases: Third Edition.* 2015;3:85–96.

81. Kuzmenko V, Sämfors S, Hägg D, Gatenholm P. Universal method for protein bioconjugation with nanocellulose scaffolds for increased cell adhesion. *Mater Sci Eng C*. 2013;33(8):4599–607.

82. Wang J, Wan YZ, Luo HL, Gao C, Huang Y. Immobilization of gelatin on bacterial cellulose nanofibers surface via crosslinking technique. *Mater Sci Eng C.* 2012;32(3):536–41.

83. Van Zyl EM, Coburn JM. Hierarchical structure of bacterial-derived cellulose and its impact on biomedical applications. *Curr Opin Chem Eng*. 2019;24:122–30.

84. Zaborowska M, Bodin A, Bäckdahl H, Popp J, Goldstein A, Gatenholm P. Microporous bacterial cellulose as a potential scaffold for bone regeneration. *Acta Biomater.* 2010;6(7):2540–7.

85. Tazi N, Zhang Z, Messaddeq Y, Almeida-Lopes L, Zanardi LM, Levinson D, et al. Hydroxyapatite bioactivated bacterial cellulose promotes osteoblast growth and the formation of bone nodules. *AMB Express.* 2012;2(1):1–10.

86. Klemm D, Schumann D, Udhardt U, Marsch S. Bacterial synthesized cellulose - Artificial blood vessels for microsurgery. *Prog Polym Sci.* 2001;26(9):1561–603.

87. Bernardelli de Mattos I, Nischwitz SP, Tuca AC, Groeber-Becker F, Funk M, Birngruber T, et al. Delivery of antiseptic solutions by a bacterial cellulose wound dressing: Uptake, release and antibacterial efficacy of octenidine and povidone-iodine. *Burns.* 2020;46(4):918–27.

88. Inoue BS, Streit S, dos Santos Schneider AL, Meier MM. Bioactive bacterial cellulose membrane with prolonged release of chlorhexidine for dental medical application. *Int J Biol Macromol.* 2020;148:1098–108.

89. Mondal S. Preparation, properties and applications of nanocellulosic materials. *Carbohydr Polym.* 2017;163:301–16.

90. Auta R, Adamus G. Production and characterization of bacterial cellulose before and after enzymatic hydrolysis. *African J Biotechnol.* 2017;16(10):470–82.

91. Zhou S, Ingram LO. Synergistic hydrolysis of carboxymethyl cellulose and acid-swollen cellulose by two endoglucanases (CelZ and CelY) from Erwinia chrysanthemi. *J Bacteriol.* 2000;182(20):5676–82.

92. Santa-Maria M, Jeoh T. Molecular-scale investigations of cellulose microstructure during enzymatic hydrolysis. *Biomacromolecules.* 2010;11(8):2000–7.

93. George J, Ramana KV, Sabapathy SN, Jagannath JH, Bawa AS. Characterization of

chemically treated bacterial (Acetobacter xylinum) biopolymer: Some thermo-mechanical properties. *Int J Biol Macromol.* 2005;37(4):189–94.

94. Choi SM, Shin EJ. The nanofication and functionalization of bacterial cellulose and its applications. *Nanomaterials.* 2020;10(3):1–24.

95. Domingues AA, Pereira F V., Sierakowski MR, Rojas OJ, Petri DFS. Interfacial properties of cellulose nanoparticles obtained from acid and enzymatic hydrolysis of cellulose. *Cellulose.* 2016;23(4):2421–37.

96. Rovera C, Fiori F, Trabattoni S, Romano D, Farris S. Enzymatic hydrolysis of bacterial cellulose for the production of nanocrystals for the food packaging industry. *Nanomaterials.* 2020;10(4):1–11.

97. Neng W, Enyong D, Rongshi C. Preparation and liquid crystalline properties of spherical cellulose nanocrystals. *Langmuir.* 2008;24(1):5–8.

98. Habibi Y. Key advances in the chemical modification of nanocelluloses. *Chem Soc Rev.* 2014;43(5):1519–42.

99. Hirai A, Inui O, Horii F, Tsuji M. Phase Separation Behavior in Aqueous Suspensions of Bacterial Cellulose Nanocrystals Prepared by Sulfuric Acid Treatment. *Langmuir.* 2009;25(1):497–502.

100. Kumar A, Singh Negi Y, Choudhary V, Kant Bhardwaj N. Characterization of Cellulose Nanocrystals Produced by Acid-Hydrolysis from Sugarcane Bagasse as Agro-Waste. *J Mater Phys Chem.* 2020;2(1):1–8.

101. Araki J, Wada M, Kuga S. Steric stabilization of a cellulose microcrystal suspension by poly(ethylene glycol) grafting. *Langmuir.* 2001;17(1):21–7.

102. Fittipaldi N, Pessoa J, Feitosa A, Miguel F, Paulo J, Morais S, et al. Bacterial cellulose nanocrystals produced under different hydrolysis conditions : Properties and morphological features. *Carbohydr Polym.* 2017;155:425–31.

103. Yan H, Chen X, Song H, Li J, Feng Y, Shi Z, et al. Food Hydrocolloids Synthesis of bacterial cellulose and bacterial cellulose nanocrystals for their applications in the

stabilization of olive oil pickering emulsion. *Food Hydrocoll*. 2017;72:127–35.

104. Arserim-Uçar DK, Korel F, Liu LS, Yam KL. Characterization of bacterial cellulose nanocrystals: Effect of acid treatments and neutralization. *Food Chem.* 2021;336:127597.

105. Salari M, Sowti Khiabani M, Rezaei Mokarram R, Ghanbarzadeh B, Samadi Kafil H. Preparation and characterization of cellulose nanocrystals from bacterial cellulose produced in sugar beet molasses and cheese whey media. *Int J Biol Macromol*. 2019;122:280–8.

106. V. F, Chanzy H. Polymer Nanocomposites Reinforced by Cellulose Whiskers. *Macromolecules.* 1995;28:6365–7.

107. Araki J, Kuga S. Effect of trace electrolyte on liquid crystal type of cellulose microcrystals. *Langmuir.* 2001;17(15):4493–6.

108. Martínez-Sanz M, Lopez-Rubio A, Lagaron JM. Optimization of the nanofabrication by acid hydrolysis of bacterial cellulose nanowhiskers. *Carbohydr Polym.* 2011;85(1):228–36.

109. Marta Martınez-Sanz, Richard T. Olsson, Amparo Lopez-Rubio JML. Development of Bacterial Cellulose Nanowhiskers Reinforced EVOH Composites by Electrospinning. *J Appl Polym Sci.* 2012;142(2):1398–408.

110. Carvalheiro F, Duarte LC, Gírio FM. Hemicellulose biorefineries: A review on biomass pretreatments. *J Sci Ind Res (India).* 2008;67(11):849–64.

111. Cherian BM, Leão AL, de Souza SF, Thomas S, Pothan LA, Kottaisamy M. Isolation of nanocellulose from pineapple leaf fibres by steam explosion. *Carbohydr Polym.* 2010;81(3):720–5.

112. Kaushik A, Singh M. Isolation and characterization of cellulose nanofibrils from wheat straw using steam explosion coupled with high shear homogenization. *Carbohydr Res.* 2011;346(1):76–85.

113. Chirayil CJ, Joy J, Mathew L, Mozetic M, Koetz J, Thomas S. Isolation and

characterization of cellulose nanofibrils from Helicteres isora plant. *Ind Crops Prod*. 2014;59:27–34.

114. Deepa B, Abraham E, Cherian BM, Bismarck A, Blaker JJ, Pothan LA, et al. Structure, morphology and thermal characteristics of banana nano fibers obtained by steam explosion. *Bioresour Technol.* 2011;102(2):1988–97.

115. Saragih SW, Wirjosentono B, Eddiyanto, Meliana Y. Influence of crosslinking agent on the morphology, chemical, crystallinity and thermal properties of cellulose nanofiber using steam explosion. *Case Stud Therm Eng.* 2020;22:100740.

116. Oliveira FMV, Pinheiro IO, Souto-Maior AM, Martin C, Gonçalves AR, Rocha GJM. Industrial-scale steam explosion pretreatment of sugarcane straw for enzymatic hydrolysis of cellulose for production of second generation ethanol and value-added products. *Bioresour Technol.* 2013;130:168–73.

117. Lima GDM, Sierakowski MR, Faria-Tischer PCS, Tischer CA. Characterisation of bacterial cellulose partly acetylated by dimethylacetamide/lithium chloride. *Mater Sci Eng C*. 2011;31(2):190–7.

118. Yudianti R, Syampurwadi A, Onggo H, Karina M, Uyama H, Azuma J. Properties of bacterial cellulose transparent film regenerated from dimethylacetamide–LiCl solution. *Polym Adv Technol.* 2016;27(8):1102–7.

119. Xu X, Liu F, Jiang L, Zhu JY, Haagenson D, Wiesenborn DP. Cellulose nanocrystals vs. Cellulose nanofibrils: A comparative study on their microstructures and effects as polymer reinforcing agents. *ACS Appl Mater Interfaces*. 2013;5(8):2999–3009.

120. Garside P, Wyeth P. Identification of cellulosic fibres by FTIR spectroscopy: Differentiation of flax and hemp by polarized ATR FTIR. *Stud Conserv.* 2006;51(3):205–11.

121. Moohan J, Stewart SA, Espinosa E, Rosal A, Rodríguez A, Larrañeta E, et al. Cellulose nanofibers and other biopolymers for biomedical applications. A review. *Appl Sci.* 2020;10(1).

122. Bhat AH, Dasan YK, Khan I, Soleimani H, Usmani A. Application of nanocrystalline cellulose: Processing and biomedical applications [Internet]. *Cellulose-Reinforced Nanofibre Composites: Production, Properties and Applications.* 2017;215–240.

123. Reiniati I, Hrymak AN, Margaritis A. Recent developments in the production and applications of bacterial cellulose fibers and nanocrystals. *Crit Rev Biotechnol.* 2017;37(4):510–24.

124. Roman M, Winter WT. Effect of Sulfate Groups from Sulfuric Acid Hydrolysis on the Thermal Degradation Behavior of Bacterial Cellulose. *Biomacromolecules.* 2004;5(5):1671–7.

125. George J, Bawa AS. Synthesis and Characterization of Bacterial Cellulose Nanocrystals and their PVA Nanocomposites. *Advanced Materials Research.* 2010;125:383–6.

126. Blanco A, Monte MC, Campano C, Balea A, Merayo N, Negro C. Nanocellulose for Industrial Use : Cellulose Nanofibers (CNF), Cellulose Nanocrystals (CNC), and Bacterial Cellulose (BC). *Handbook of Nanomaterials for Industrial Applications.* 2018. 74–126.

127. Chen XI. Degradation Studies on Plant Cellulose and Bacterial Cellulose by FT-IR and ESEM. Master Thesis, University of Birmingham, 2014, UK.

APPENDIX A

The preparation of bacterial cellulose samples can be seen below images. Bacterial celulose pellicle was treated with with 2M NaOH at 80°C for 1h, and it was broken into pieces then pretreated with different concentration of sulphuric acid as can be seen Figure A.1.

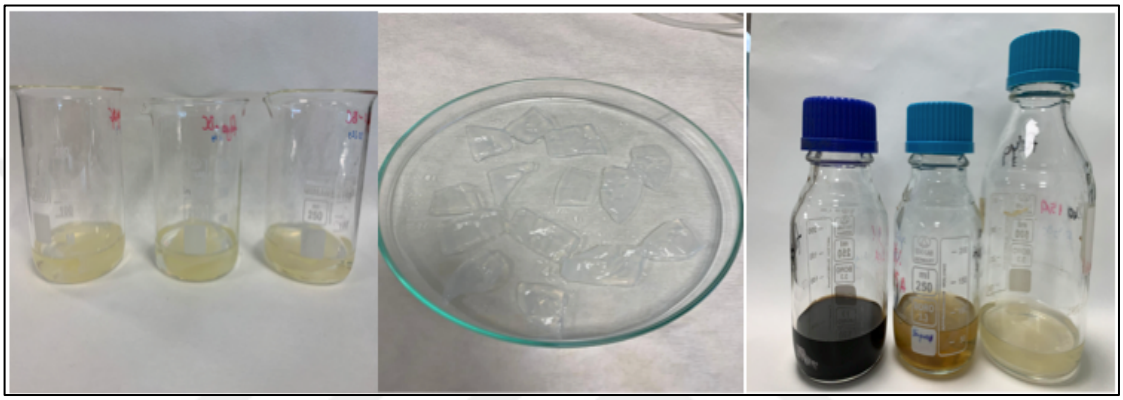

Figure A.1. Experimental set-up a) bacterial cellulose pellicle was treated with 2M NaOH at 80°C for 1h b) bacterial cellullose pellicle was broken into pieces c)sulphuric acid pretreatment with autoclave (90% sulphuric acid left; 65% sulphuric acid middle; 40% sulphuric acid left)

After the pretreatments and degradation processes, the images of samples can be seen Figure A.2., Figure A.3., Figure A.4. and Figure A.5. There are remarkable differences between Figure A.2., Figure A.3. and Figure A.4.

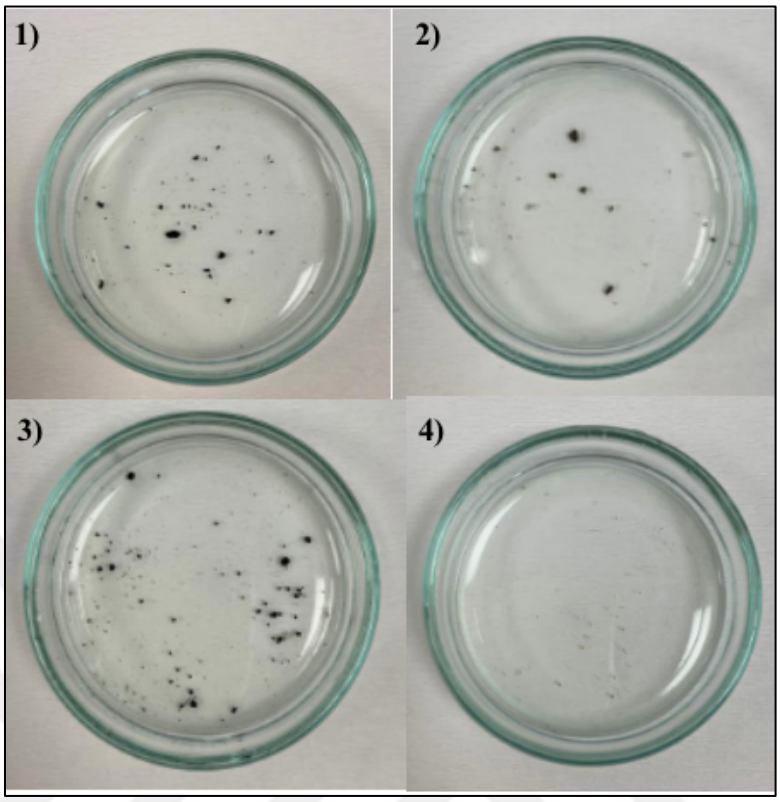

Figure A.2. Images of samples after treatments 1) 90% sulphuric acid pretretament with autoclave 15 min and degraded with 65% sulphuric acid at room temperature for 2 days 2) 90% sulphuric acid pretreatment at room temperature 1h 40 min and degraded with 65% sulphuric acid at room temperature for 2 days 3) 90% sulphuric acid pretretament with autoclave 45 min and degraded with 65% sulphuric acid at room temperature for 2 days 4) 90% sulphuric acid pretreatment at room temperature 2h 40 min and degraded with 65% sulphuric acid at room temperature for 2 days

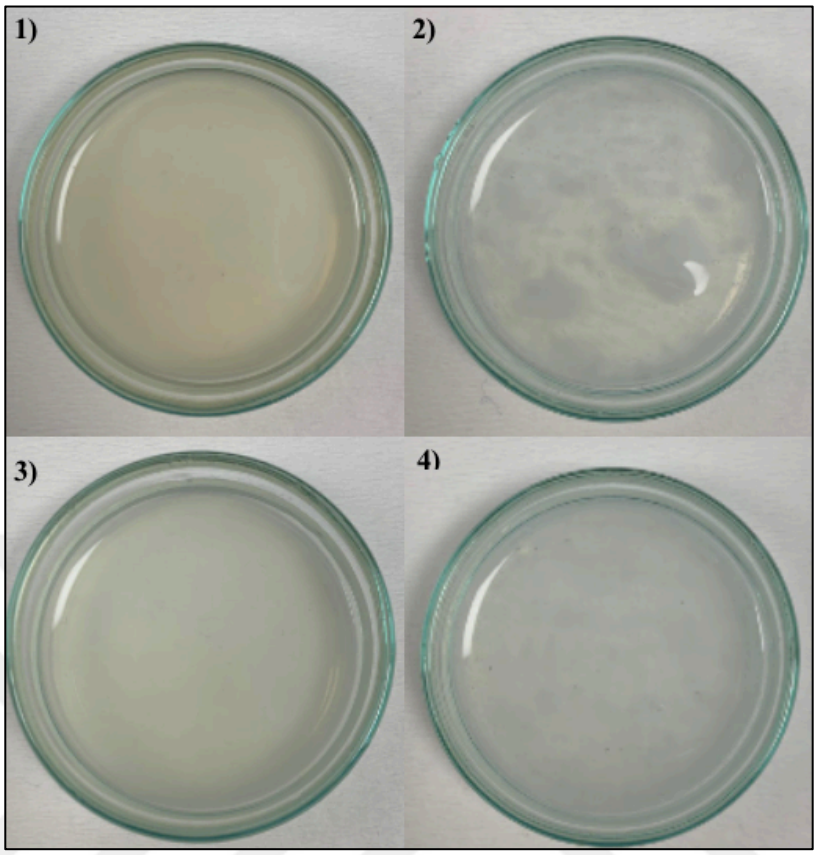

Figure A.3. Images of samples after treatments 1) 65% sulphuric acid pretretament with autoclave 45 min and degraded with 65% sulphuric acid at room temperature for 2 days 2) 65% sulphuric acid pretreatment at room temperature 2h 40 min and degraded with 65% sulphuric acid at room temperature for 2 days 3) 65% sulphuric acid pretretament with autoclave 15 min and degraded with 65% sulphuric acid at room temperature for 2 days 4) 65% sulphuric acid pretreatment at room temperature 1h 40 min and degraded with 65% sulphuric acid at room temperature for 2 days

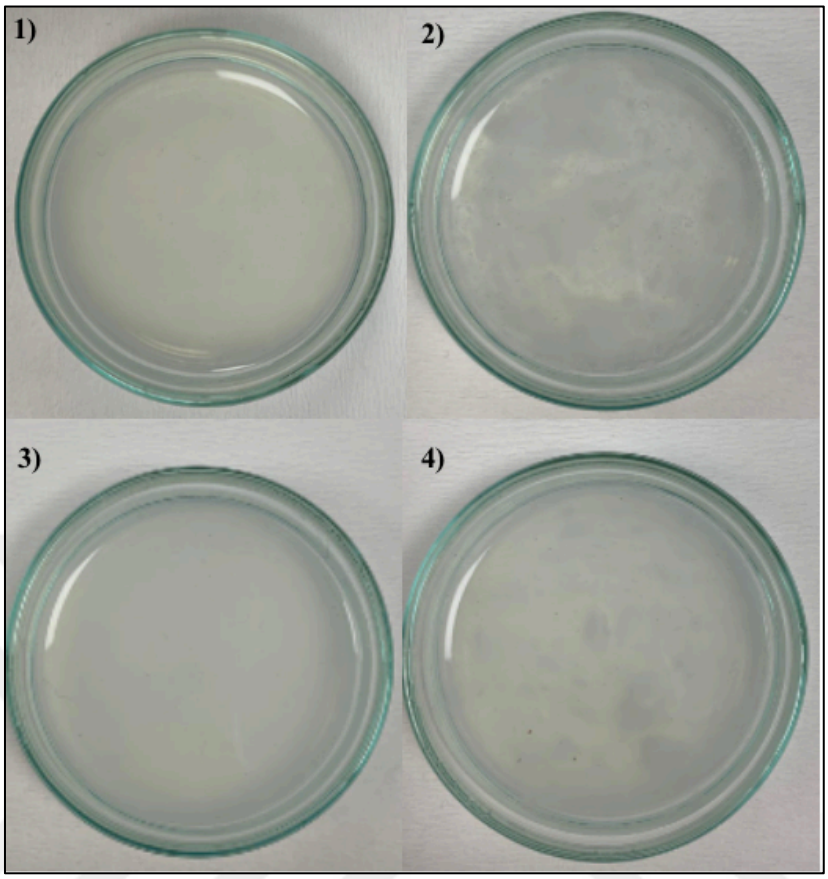

Figure A.4. Images of samples after treatments 1) 40% sulphuric acid pretretament with autoclave 45 min and degraded with 65% sulphuric acid at room temperature for 2 days 2) 40% sulphuric acid pretreatment at room temperature 2h 40 min and degraded with 65% sulphuric acid at room temperature for 2 days 3) 40% sulphuric acid pretretament with autoclave 15 min and degraded with 65% sulphuric acid at room temperature for 2 days 4) 40% sulphuric acid pretreatment at room temperature 1h 40 min and degraded with 65% sulphuric acid at room temperature for 2 days

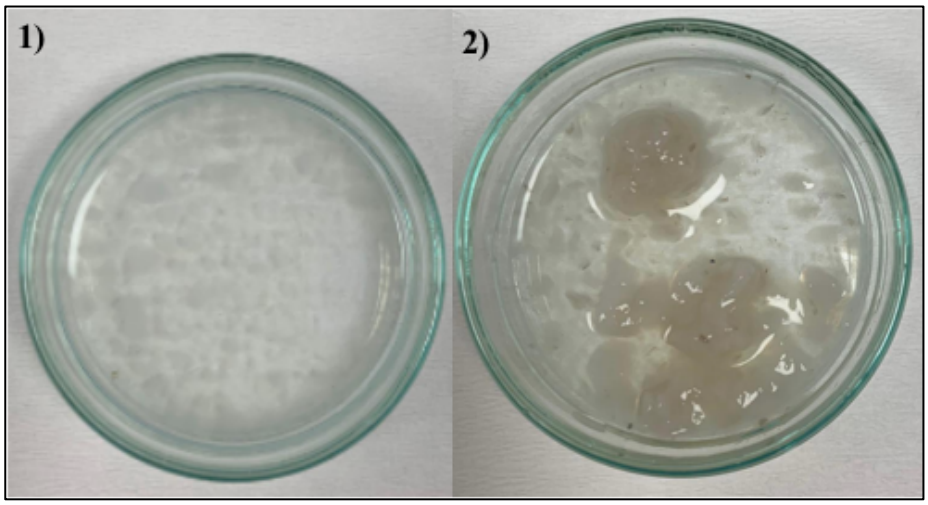

Figure A.5. Images of samples after treatments 1) 8% (w/v) pretreatment with LiCl-DMA and degradation with Liquid nitrogen 2) 8% (w/v) pretreatment with LiCl-DMA and treatment with 40% sulphuric acid with autoclave 15 min

APPENDIX B

The spectra of all samples were analyzed between 525cm^{-1} and 4000 cm^{-1}.

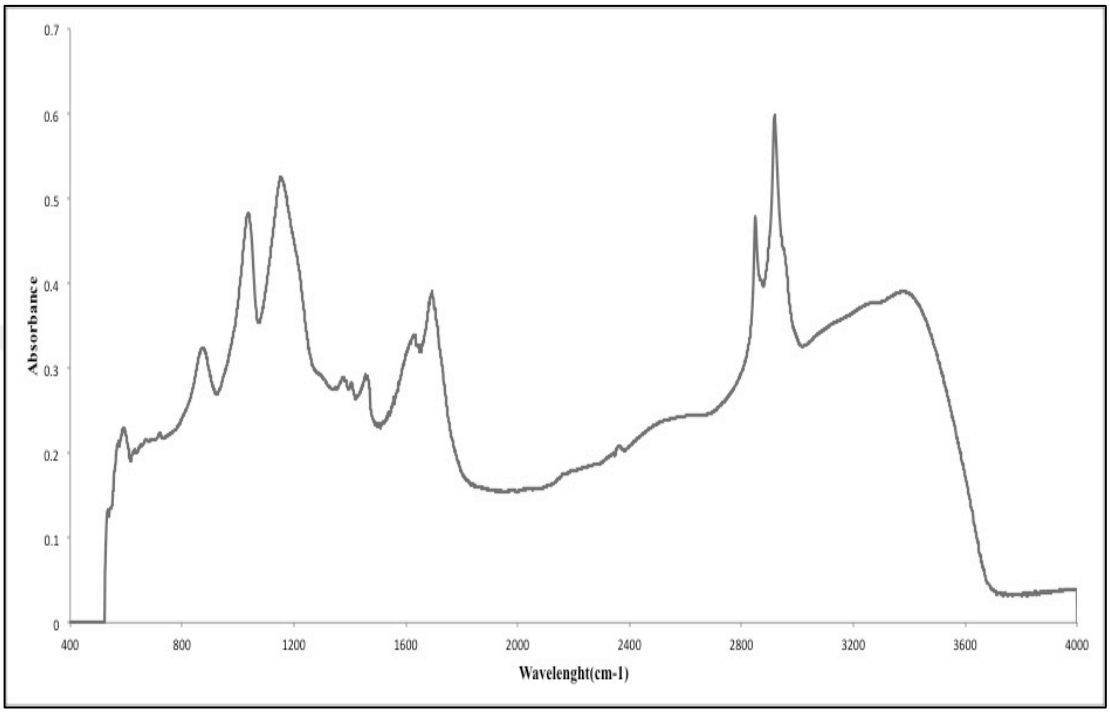

Figure B.1. FT-IR spectrum for 90% sulphuric acid pretreatment with autoclave for 45 min at 121°C and degradation with 65% sulphuric acid at room temperature for 2 days

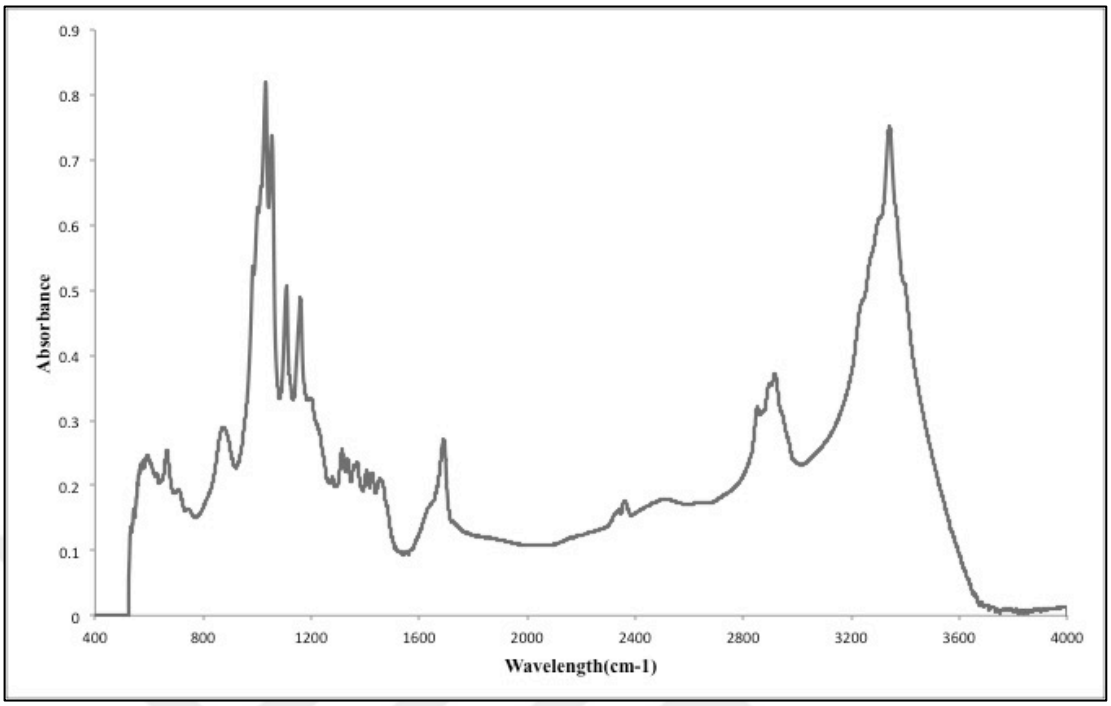

Figure B.2. FT-IR spectrum for 65% sulphuric acid pretreatment with autoclave for 45 min at 121°C and degradation with 65% sulphuric acid at room temperature for 2 days

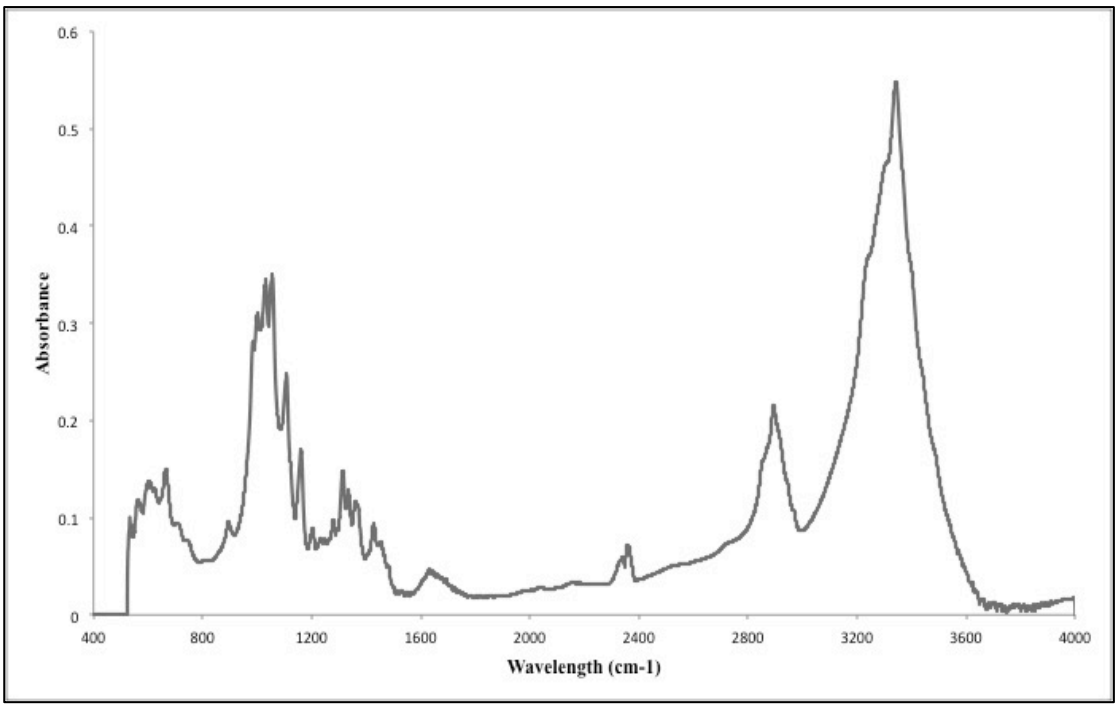

Figure B.3. FT-IR spectrum for 40% sulphuric acid pretreatment with autoclave for 45 min at 121°C and degradation with 65% sulphuric acid at room temperature for 2 days

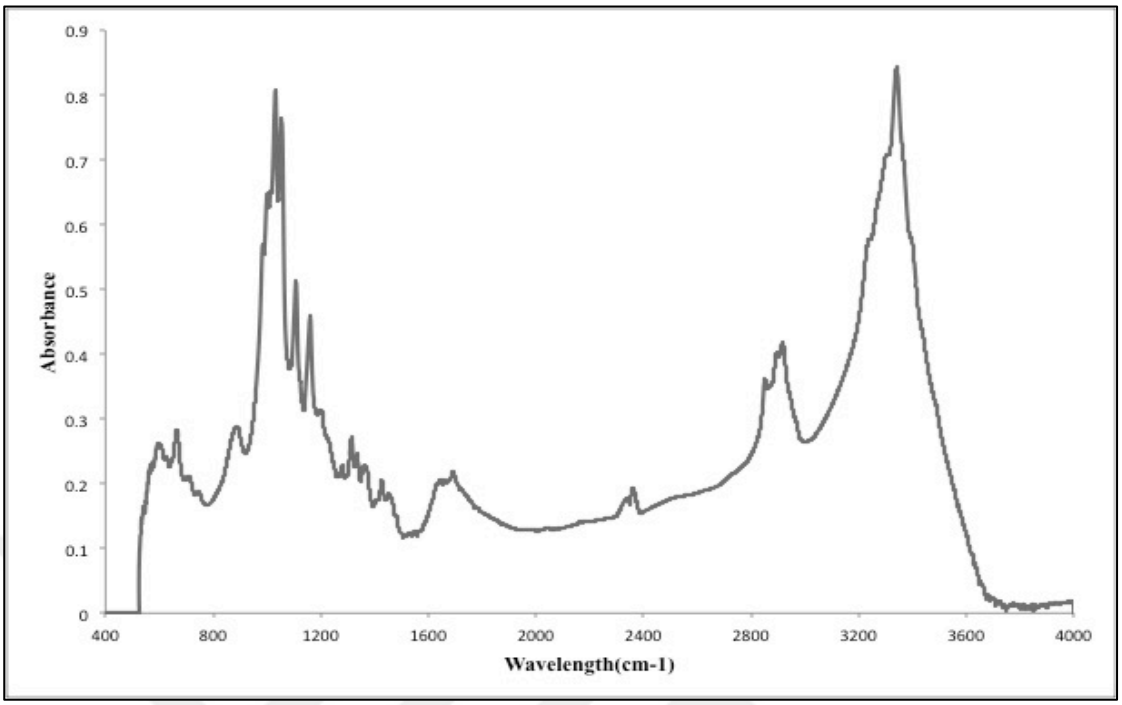

Figure B.4. FT-IR spectrum for 90% sulphuric acid pretreatment at room temperature for 2 hours 40 min and degradation with 65% sulphuric acid at room temperature for 2 days

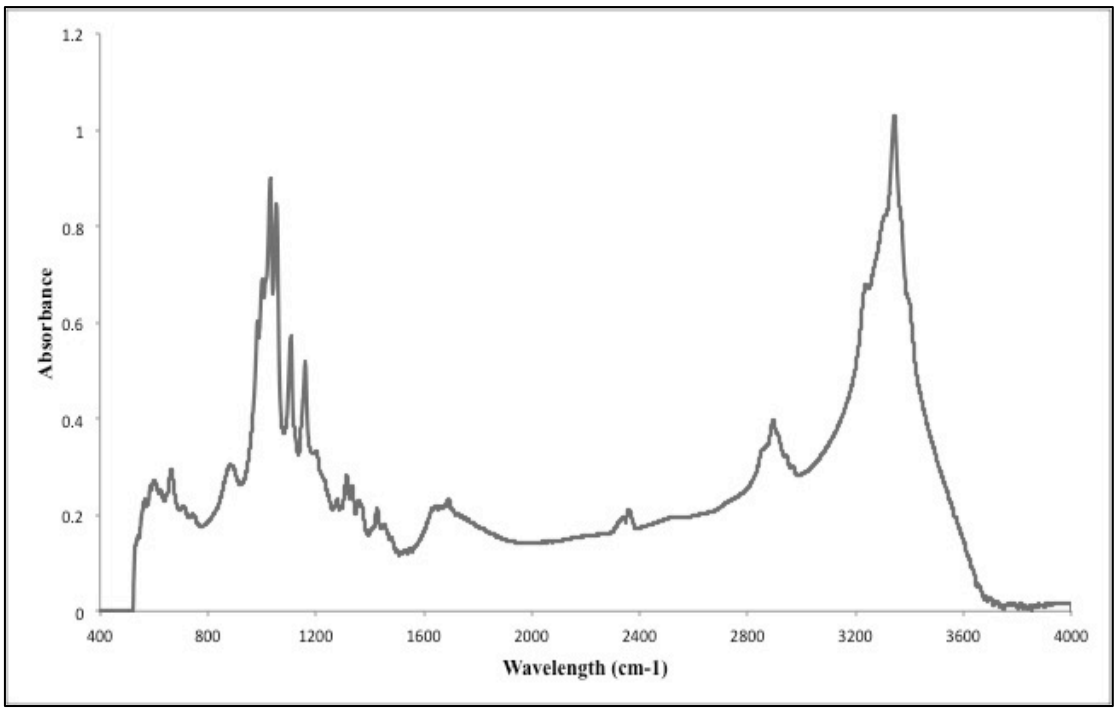

Figure B.5. FT-IR spectrum for 65% sulphuric acid pretreatment at room temperature for 2 hours 40 min and degradation with 65% sulphuric acid at room temperature for 2 days

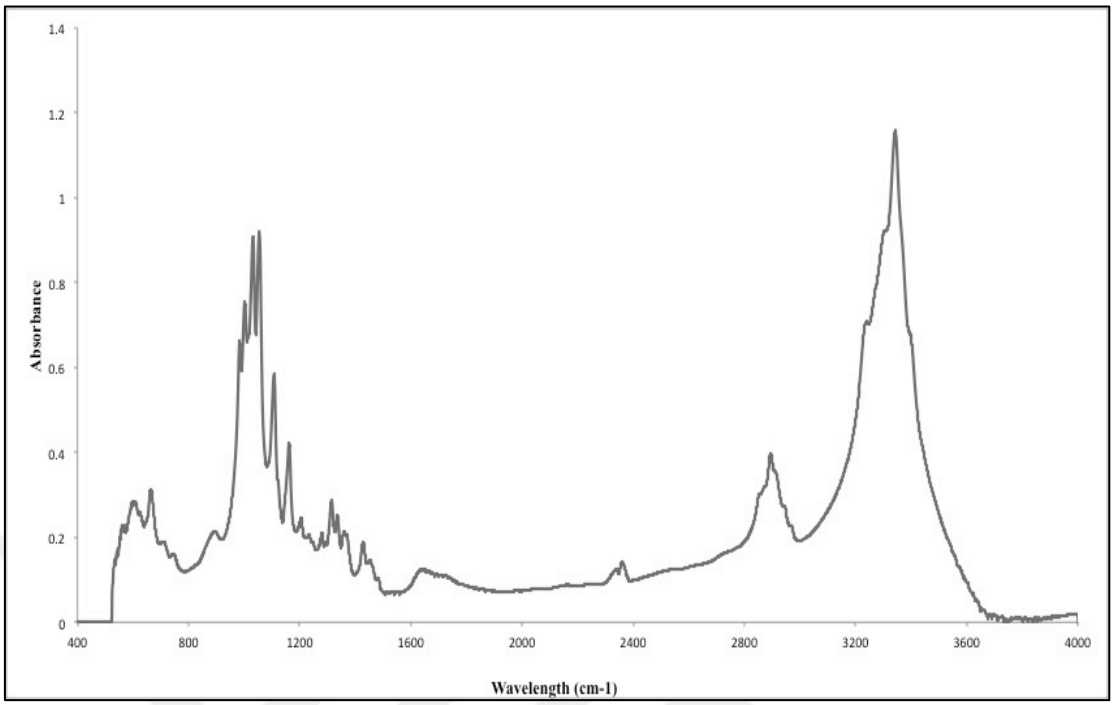

Figure B.6. FT-IR spectrum for 40% sulphuric acid pretreatment at room temperature for 2 hours 40 min and degradation with 65% sulphuric acid at room temperature for 2 days

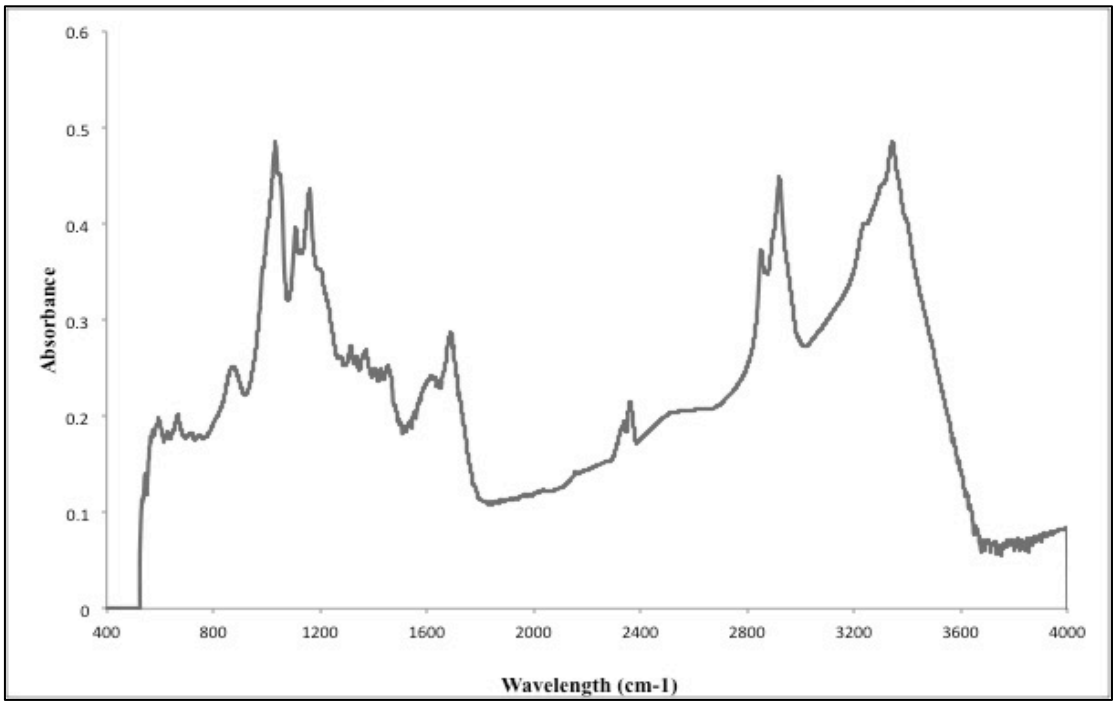

Figure B.7. FT-IR spectrum for 90% sulphuric acid pretreatment with autoclave for 15 min at 121°C and degradation with 65% sulphuric acid at room temperature for 2 days

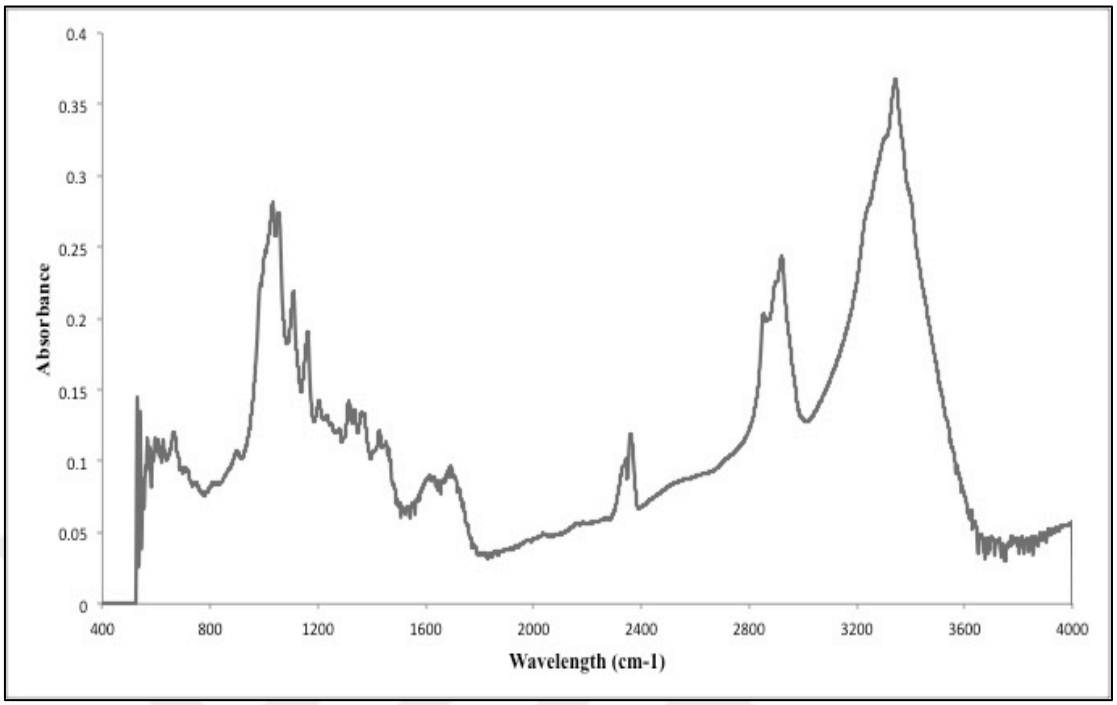

Figure B.8. FT-IR spectrum for 65% sulphuric acid pretreatment with autoclave for 15 min at 121°C and degradation with 65% sulphuric acid at room temperature for 2 days

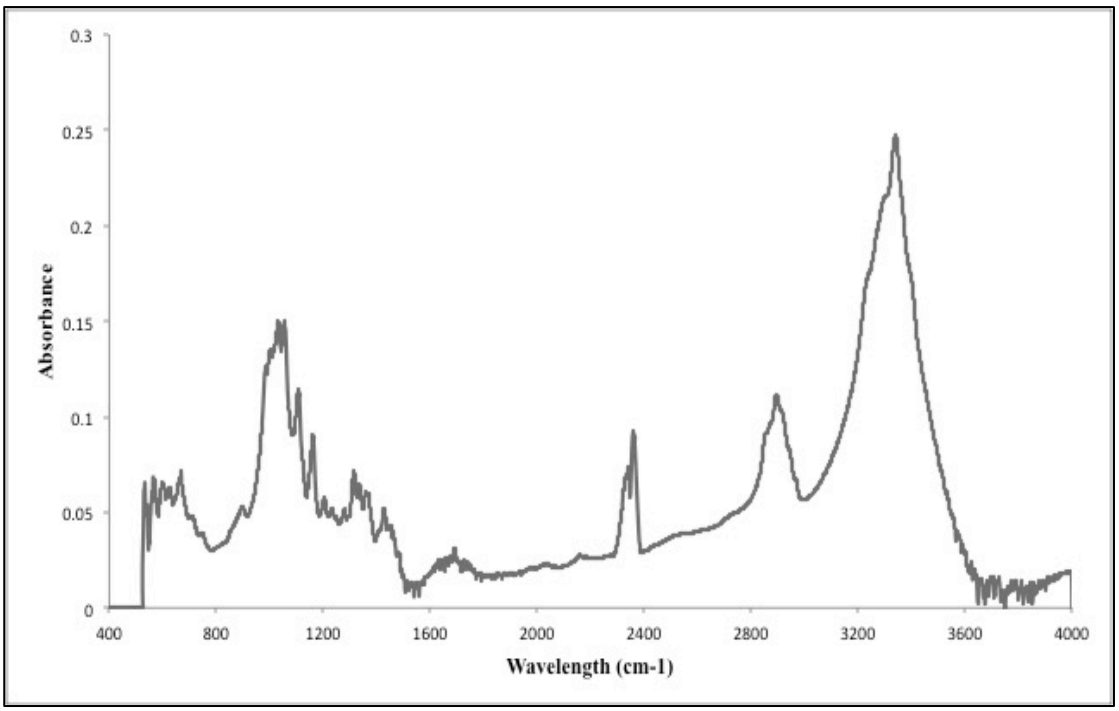

Figure B.9. FT-IR spectrum for 40% sulphuric acid pretreatment with autoclave for 15 min at 121°C and degradation with 65% sulphuric acid at room temperature for 2 days

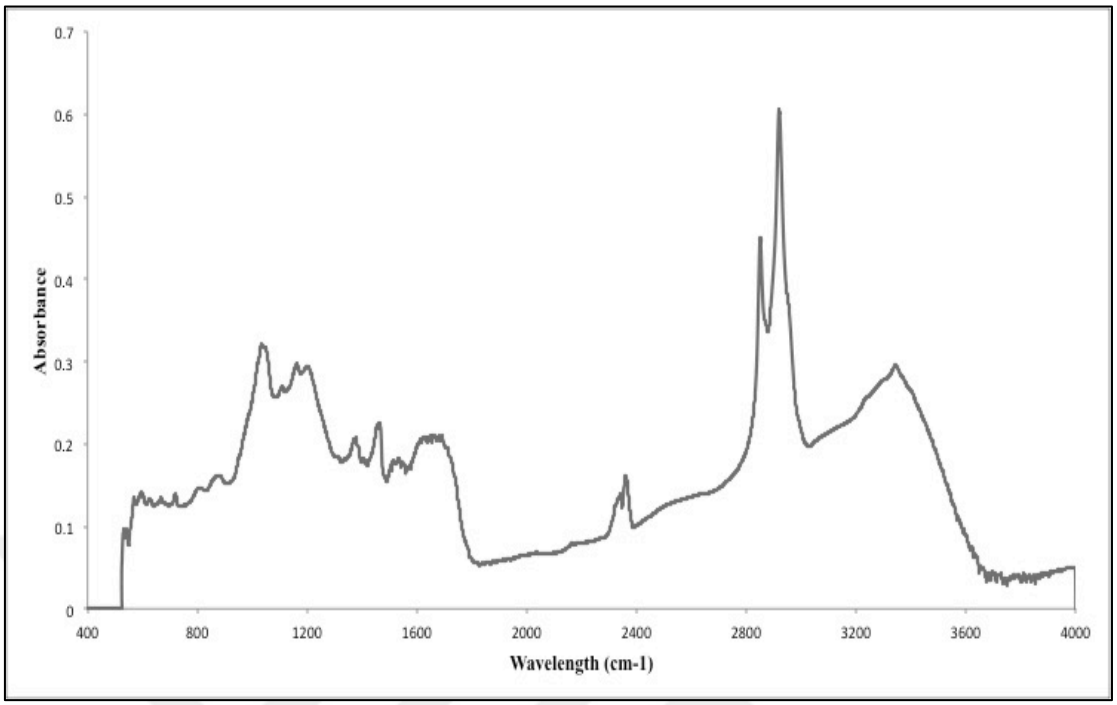

Figure B.10. FT-IR spectrum for 90% sulphuric acid pretreatment at room temperature for 1 hour 40 min and degradation with 65% sulphuric acid at room temperature for 2 days

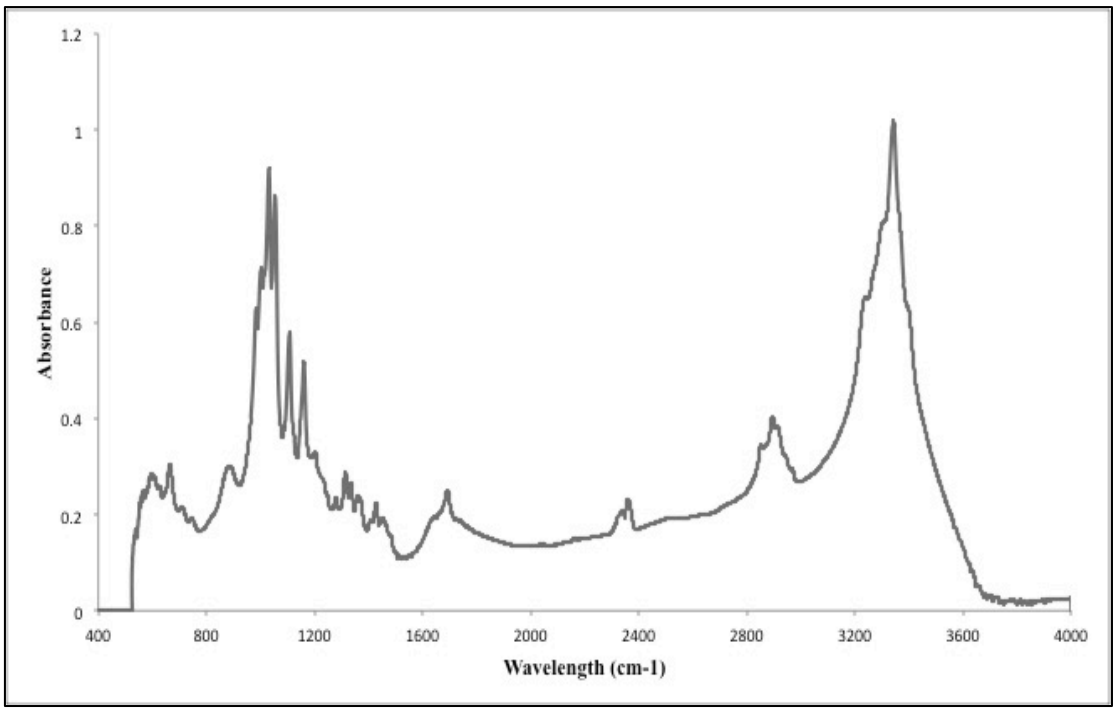

Figure B.11. FT-IR spectrum for 65% sulphuric acid pretreatment at room temperature for 1 hour 40 min and degradation with 65% sulphuric acid at room temperature for 2 days

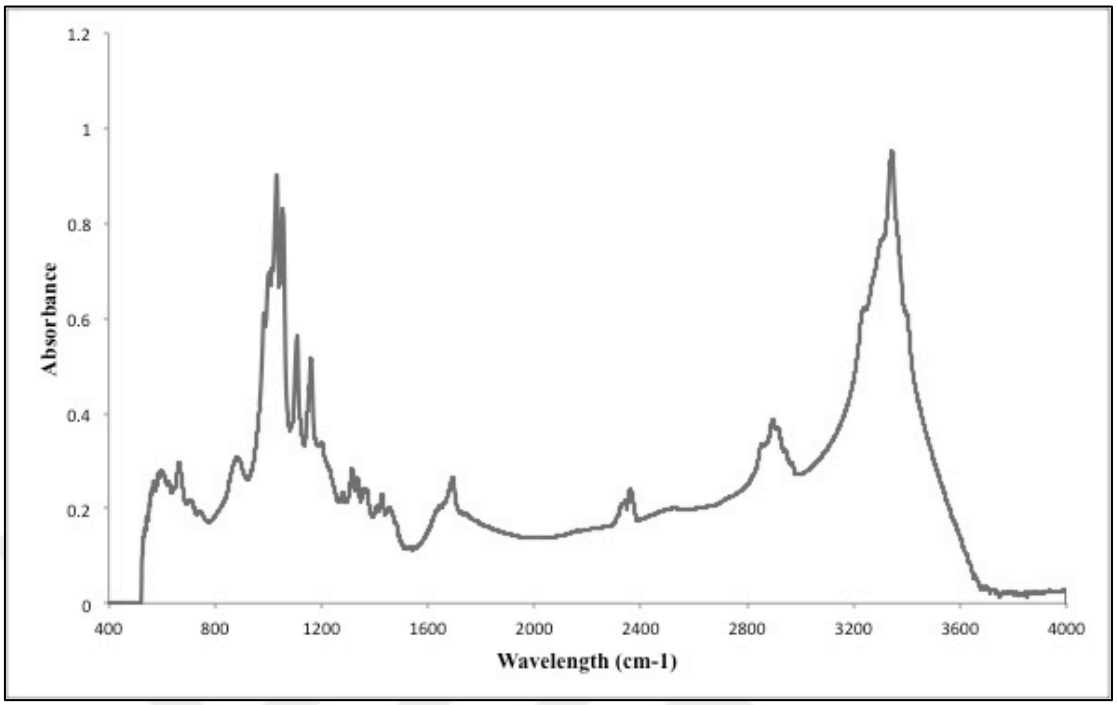

Figure B.12. FT-IR spectrum for 40% sulphuric acid pretreatment at room temperature for 1 hour 40 min and degradation with 65% sulphuric acid at room temperature for 2 days

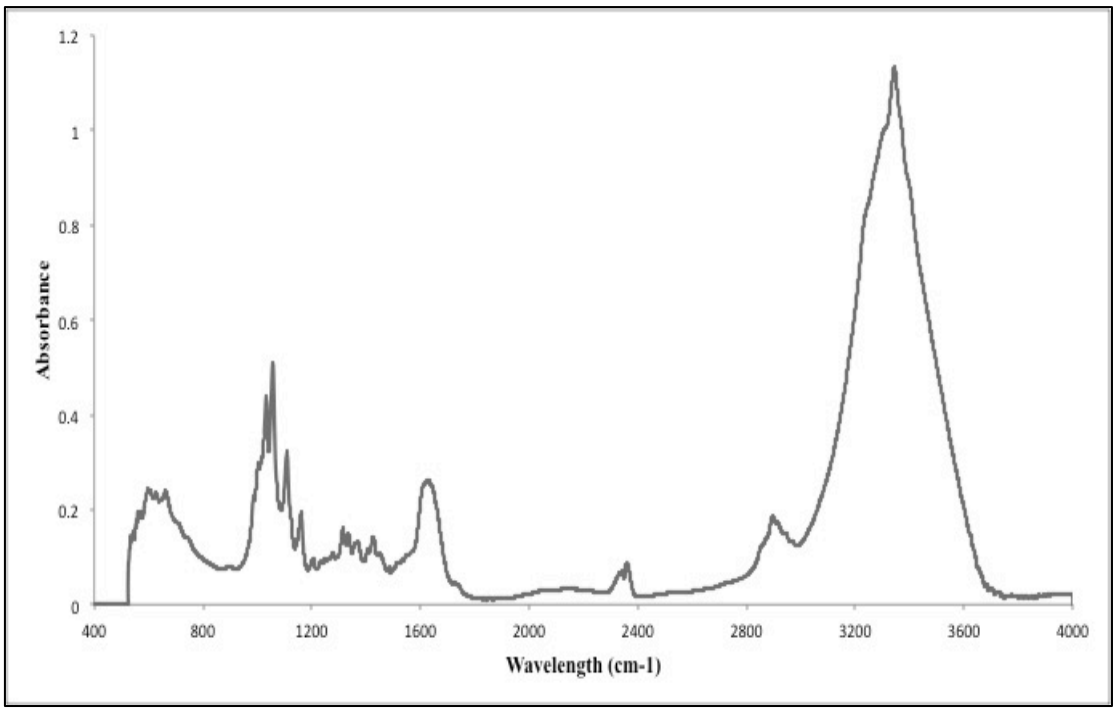

Figure B.13. FT-IR spectrum for 8% (w/v) LiCL-DMA pretreatment for 2 days at room temperature and degradation with liquid nitrogen

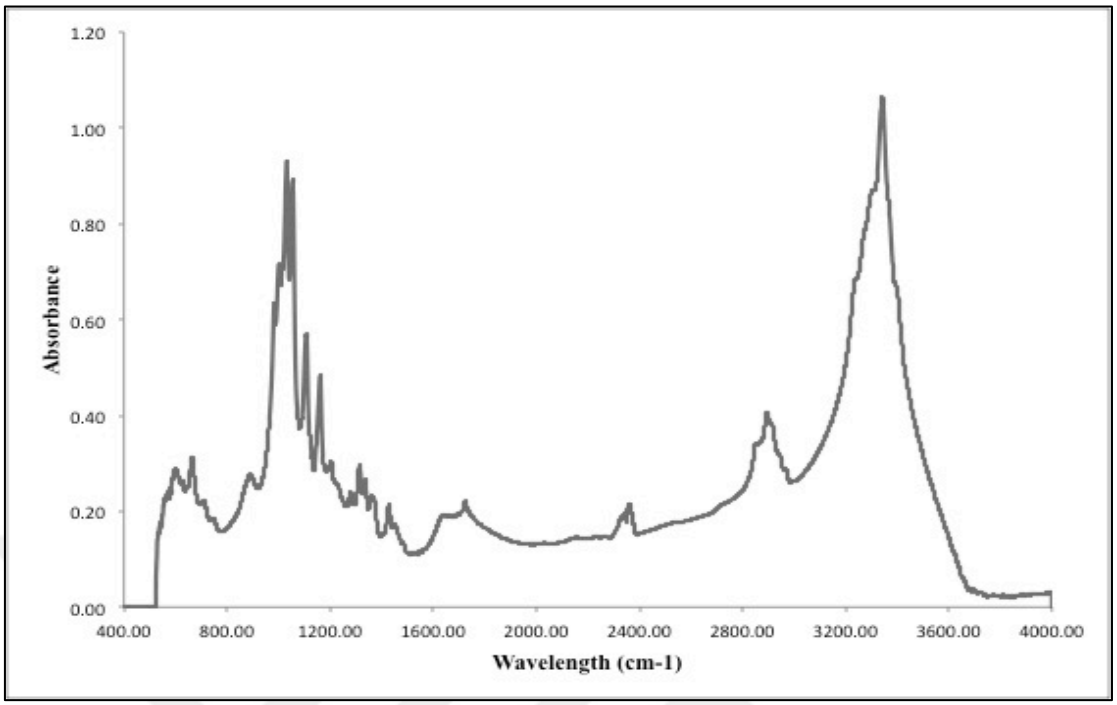

Figure B.14. FT-IR spectrum for 8% (w/v) LiCL-DMA pretreatment for 2 days at room temperature and treated with 40% sulphuric acid with autoclave for 15 min at 121°C

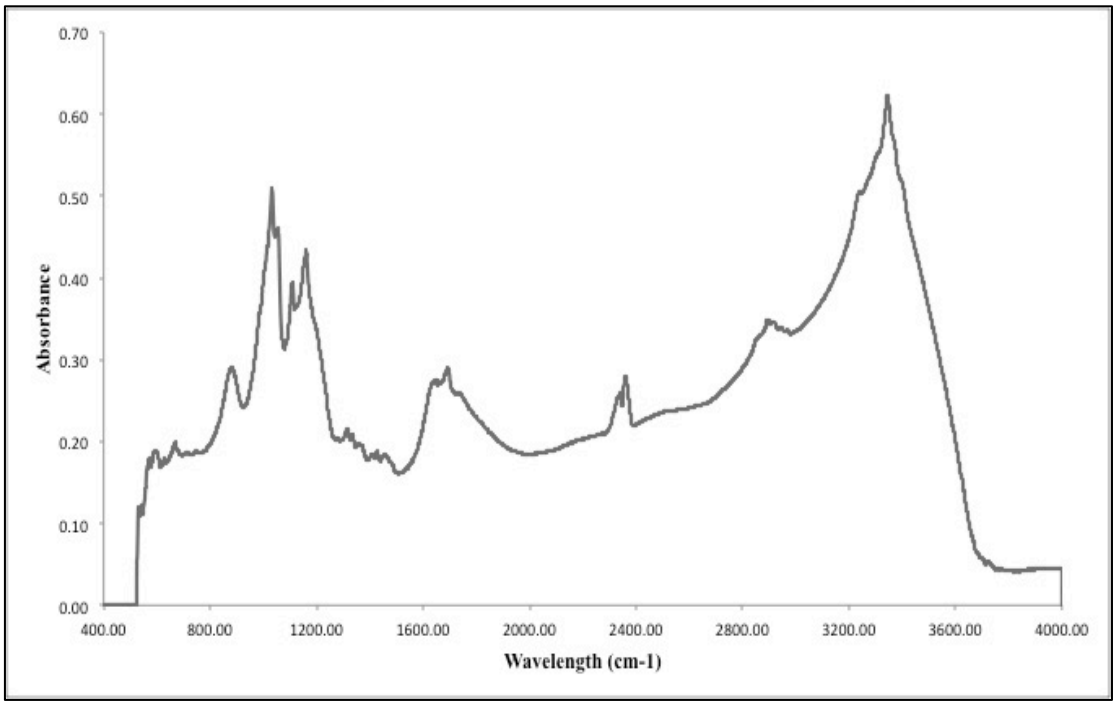

Figure B.15. FT-IR spectrum of pretreatment for 65% sulphuric acid at room temperature for 2 days

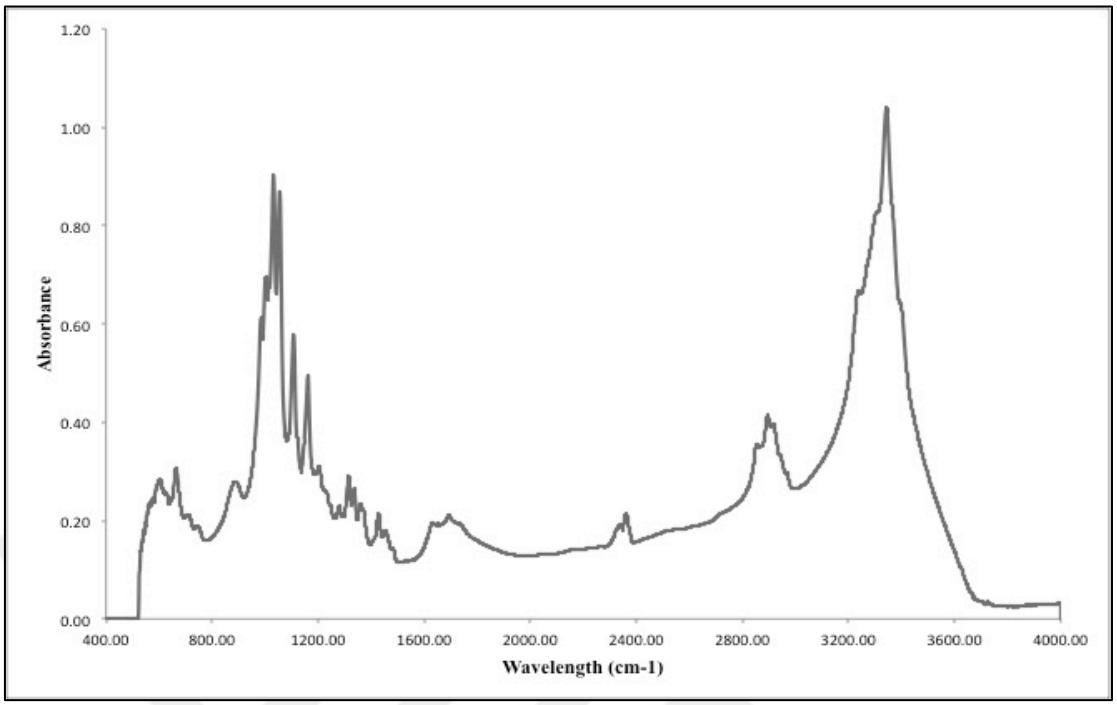

Figure B.16. FT-IR spectrum of pretreatment for 40% sulphuric acid with autoclave for 15 min at 121°C